Department of Signal Processing and Acoustics

Measurements, analysis and modeling of wind-driven ambient noise in shallow brackish water

Ari Poikonen

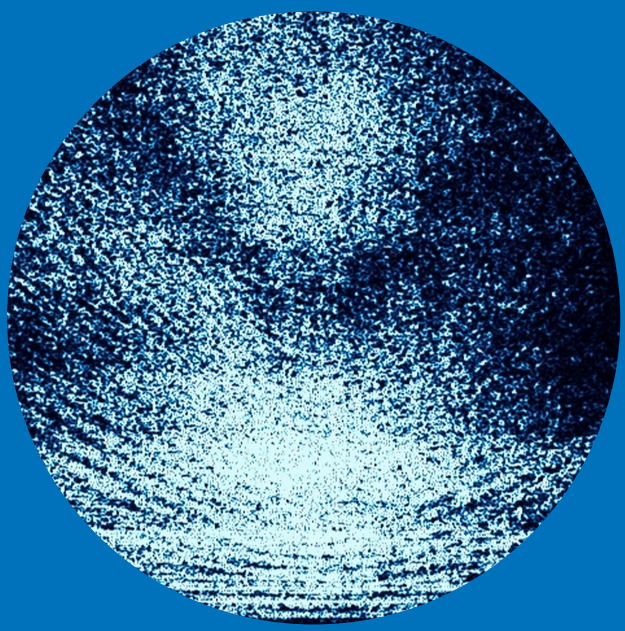

Aalto University

DOCTORAL DISSERTATIONS

Aalto University publication series
DOCTORAL DISSERTATIONS 18/2012

Measurements, analysis and modeling of wind-driven ambient noise in shallow brackish water

Ari Poikonen

Doctoral dissertation for the degree of Doctor of Science in Technology to be presented with due permission of the School of Electrical Engineering for public examination and debate in Auditorium S1 at the Aalto University School of Electrical Engineering (Espoo, Finland) on the 9th of March 2012 at 12 noon.

Aalto University
School of Electrical Engineering
Department of Signal Processing and Acoustics

Supervisor
Prof. Unto K. Laine, Aalto University, Finland

Instructor
Dr. Martti Kalliomäki (ret.), Finnish Naval Research Institute, Finland

Preliminary examiners
Prof. Pekka Heikkinen, University of Helsinki, Finland
Dr. Seppo Uosukainen, Technical Research Centre of Finland (VTT), Finland

Opponent
Dr. Jörgen Pihl, Swedish Defence Research Agency (FOI), Sweden

Aalto University publication series
DOCTORAL DISSERTATIONS 18/2012

ISBN 978-952-60-4513-9 (printed)
ISBN 978-952-60-4514-6 (pdf)
ISSN-L 1799-4934
ISSN 1799-4934 (printed)
ISSN 1799-4942 (pdf)

Unigrafia Oy
Helsinki 2012

Finland

The dissertation can be read at http://lib.tkk.fi/Diss/

441 697
Printed matter

Author
Ari Poikonen

Name of the doctoral dissertation
Measurements, analysis and modeling of wind-driven ambient noise in shallow brack-ish water

Publisher School of Electrical Engineering

Unit Department of Signal Processing and Acoustics

Series Aalto University publication series DOCTORAL DISSERTATIONS 18/2012

Field of research Underwater acoustics

Manuscript submitted 30 May 2011 **Manuscript revised** 21 October 2011

Date of the defence 9 March 2012 **Language** English

☐ **Monograph** ☒ **Article dissertation (summary + original articles)**

Abstract

Underwater ambient noise measurements were conducted in shallow brackish water environments in the Gulf of Finland over a frequency range from 20 Hz to 70 kHz. The ambient noise levels are in fairly good agreement with average oceanic deep water levels for the highest wind speeds but the wind speed dependences differ markedly from each other. In shallow brackish water the wind speed dependence factor at 200 Hz is ~ 2.4 which is significantly higher than the typical factor of ~ 1.5 for the ocean environment. The high-frequency behavior of the spectra was resolved by modeling dispersion and noise in bubbly water. Absorption in brackish and fresh water, unlike in ocean water, tends to decrease above a frequency of 10 kHz due to the low proportion of small bubbles in bubbly mixtures created by breaking waves. The excess high-frequency attenuation in spectra above 10 kHz cannot therefore be attributed to the effects of absorption in a bubbly mixture. Bubble size distributions fitted to the brackish water spectra exhibit a distinctive maximum in the radius range 0.1 - 0.3 mm, and a substantial drop in bubble density below a radius of 0.1 mm. The brackish water bubble size distributions were tied to an oceanic spectrum with a spectral slope of 5.7 dB/octave obtained with a -3/2 power law dependence of bubble size density on radius. The measurements were carried out in all four seasons of the year but no significant seasonal effects were found in any parameter calculated from the spectra. This is probably due to the dominance of near field conditions in the measurements, where the role of long-range propagation effects was negligible. One should, however, be careful not to generalize the present brackish water results too much due to the inherent complexity of the coastal situation. Bubble densities are known to have considerable spatial variability depending on seasonal, biological, and even weather conditions.

Keywords Underwater acoustics, ambient noise, bubbles, hydrophones, sonar, Baltic Sea, Gulf of Finland

ISBN (printed) 978-952-60-4513-9 **ISBN (pdf)** 978-952-60-4514-6

ISSN-L 1799-4934 **ISSN (printed)** 1799-4934 **ISSN (pdf)** 1799-4942

Location of publisher Espoo **Location of printing** Helsinki **Year** 2012

Pages 54 **The dissertation can be read at** http://lib.tkk.fi/Diss/

Tekijä
Ari Poikonen

Väitöskirjan nimi
Tuulen matalassa murtovedessä aiheuttaman vedenalaisen kohinan mittaus, analyysi ja mallinnus

Julkaisija Sähkötekniikan korkeakoulu

Yksikkö Signaalinkäsittelyn ja akustiikan laitos

Sarja Aalto University publication series DOCTORAL DISSERTATIONS 18/2012

Tutkimusala Vedenalainen akustiikka

Käsikirjoituksen pvm 30.05.2011 **Korjatun käsikirjoituksen pvm** 21.10.2011

Väitöspäivä 09.03.2012 **Kieli** Englanti

☐ **Monografia** ☒ **Yhdistelmäväitöskirja (yhteenveto-osa + erillisartikkelit)**

Tiivistelmä

Tuulen aiheuttamaa vedenalaista kohinaa tutkittiin Suomenlahden matalissa murtovesissä taajuusalueella 20 Hz – 70 kHz. Mitattujen kohinaspektrien taso yhtyy voimakkaimmilla tuulilla muutaman desibelin tarkkuudella valtamerien keskimääräisiin kohinatasoihin, mutta kohinan tuuliriippuvuudet eroavat merkittävästi toisistaan. Matalassa murtovedessä kohinatason tuuliriippuvuuden potenssi taajuudella 200 Hz on n. 2.4, kun se on valtameriympäristössä on tyypillisesti n. 1.5. Kohinaspektrin käyttäytymistä suuremmilla taajuuksilla (yli 1 kHz) mallinnettiin sekä kuplaisen nesteen dispersiomallilla että resonanssitaajuuksillaan värähtelevien kuplien mallilla. Toisin kuin valtameressä, makeassa ja vähäsuolaisessa vedessä absorptio alkaa laskea yli 10 kHz taajuudella johtuen murtuvien aaltojen synnyttämien pienten kuplien vähäisestä suhteellisesta määrästä. Kohinaspektreissä yli 10 kHz taajuuksilla havaittua jyrkkää vaimenemista ei siten voida selittää kuplavaimennuksella. Murtovedestä mitattuihin kohinaspektreihin sovitetuissa kuplakokojakaumissa on selkeä maksimi kuplan säteillä 0.1 - 0.3 mm ja huomattava pudotus alle 0.1 mm säteillä. Murtoveden kuplakokojakaumat sidottiin valtameren vertailujakaumaan, jossa jakauman jyrkkyyden potenssi oli -3/2, joka aiheutti spektrin laskevalle osalle jyrkkyyden 5.7 dB/oktaavi. Kohinamittauksia tehtiin kaikkina vuodenaikoina, mutta ajallista riippuvuutta ei havaittu spektreistä lasketuissa parametrissä. Tämä johtuu todennäköisesti mittausten lähikenttäolosuhteista, jossa kaukaa edenneen äänen osuus on vähäinen. Rannikon olosuhteiden luontainen vaihtelu on kuitenkin suurta ja kuplakokojakaumalla tiedetään olevan huomattavaa paikallista vaihtelua, joka riippuu vuodenajasta, biologisista tekijöistä ja jopa säästä. Tämän takia mittausten johtopäätökset ovat luonteeltaan suuntaa antavia, eikä niitä tule siten liiaksi yleistää.

Avainsanat Vedenalainen akustiikka, vedenalainen kohina, kuplat, hydrofonit, kaikumittaus, Itämeri, Suomenlahti

ISBN (painettu) 978-952-60-4513-9 **ISBN (pdf)** 978-952-60-4514-6

ISSN-L 1799-4934 **ISSN (painettu)** 1799-4934 **ISSN (pdf)** 1799-4942

Julkaisupaikka Espoo **Painopaikka** Helsinki **Vuosi** 2012

Sivumäärä 54 **Luettavissa verkossa osoitteessa** http://lib.tkk.fi/Diss/

Preface

Even today, a substantial part of research on underwater acoustics world wide takes place behind the curtain of secrecy. Environmentally oriented studies, however, make an exception, where the results of naval research can be shared with civilian applications without jeopardizing information security. The present study deals with wind-driven underwater ambient noise, which is of great importance both in naval and civilian applications. The study behind this thesis was conducted in the Finnish Naval Research Institute (FNRI) between 2006 and 2011. I express my warmest gratitude to my colleague and co-author Mr. Seppo Madekivi for excellent collaboration, and for his valuable comments in testing new ideas. I would also like to thank my superiors Ph.D. Martti Kalliomäki and Navy Capt. (Eng.) Pekka Kannari for encouraging me to jump for a while from a day-to-day administrative treadmill back to the inspiring academic world, which I thought I had left behind a long time ago. I have not regretted my choice.

When I for the first time brought my scientific material to School of Electrical Engineering for initial evaluation, I got acquainted with Professor Unto K. Laine, who later on became the supervisor of my thesis. I soon recognized that we share a multidisciplinary approach to problem solving, which made it easy for us to discuss questions of a mixed discipline of underwater acoustics. I am grateful to him for inspiring and fruitful discussions during the preparation of the overview, and for coaching me back to academia. I am also indebted to the preliminary examiners D.Sc.(Tech.) Seppo Uosukainen and Prof. Pekka Heikkinen for their valuable comments on the manuscript.

Finally, I thank the members of my family for their support and encouragement, and for their patience they showed during those numerous evening hours when their ‘Earth’s calling’ messages reverberated in the study without reaching my conscious mind.

Helsinki, September 2011
Ari Poikonen

List of Publications

The thesis consists of an overview and the following publications:

I Ari Poikonen, and Seppo Madekivi, "Recent hydroacoustic measurements and studies in the Gulf of Finland", In *Proceedings of the 1st International Conference on Underwater Acoustic Measurement: Technologies and Results (UAM 2005)*, Heraklion, Greece, June 28-July 1, 2005.

II Ari Poikonen, and Seppo Madekivi, "Underwater noise measurements in very shallow coastal environment", In *Proceedings of the 2nd International Conference on Underwater Acoustic Measurement: Technologies and Results (UAM 2007),* Heraklion, Greece, June 25-29, 2007.

III Ari Poikonen, and Seppo Madekivi, "Wind-generated ambient noise in a shallow brackish water environment in the archipelago of the Gulf of Finland*", Journal of the Acoustical Society of America (JASA)*, Vol. 127, No. 6, June 2010.

IV Ari Poikonen, "High-frequency measurements of underwater ambient noise in shallow brackish water", ", In *Proceedings of the 10th European Conference on Underwater Acoustics (ECUA 2010),* Istanbul, Turkey, July 5-9, 2010.

V Ari Poikonen, "High-frequency wind-driven ambient noise in shallow brackish water: Measurements and spectra*", Journal of the Acoustical Society of America Express Letters (JASA-EL)*, Vol. 128, No. 5, October 2010.

VI Ari Poikonen, "Analysis of high-frequency wind-driven ambient noise in shallow brackish water", *Journal of the Acoustical Society of America Express Letters (JASA-EL)*, Vol. 129, No. 4, March 2011.

Author's Contribution

Publication I: Planning and compilation of the paper was done in collaboration with the co-author. The first author is responsible for studies on optimizing sonar parameters in a shallow water environment.

Publication II: The first author of the paper is mainly responsible for this research. The present author designed the measuring system and the data processing software, and wrote the draft of the paper.

Publication III: The first author of the paper is mainly responsible for this research. The present author performed the data processing, introduced the noise models, and wrote the draft of the paper.

Publication IV-VI: The present author is responsible for these publications.

Contents

List of Abbreviations

ABL	Atmospheric Boundary Layer
CTD	Conductivity, Temperature and Depth profile (vertical) in sea water
dB//µPa/√Hz	Sound spectrum level in decibel re micropascal in a 1-Hz band
EE	Echo Excess (dB) in Sonar Equation
FN	Finnish Navy
FNRI	Finnish Naval Research Institute (Merivoimien tutkimuslaitos)
FOI	Totalförsvarets Forskningsinstitut (Swedish Defence Research Agency)
GOF	Gulf of Finland
GTK	Geologian tutkimuskeskus (Geological Survey of Finland)
HF	High-frequency (f > 10 kHz)
IL	Sound Intensity Level (L_I) in hydroacoustics
MF	Medium-frequency (f = 1-10 kHz)
NL	Noise level (dB//µPa or dB//µPa/√Hz) in Sonar Equation
SL	Source Level (dB//µPa or dB//µPa/√Hz) in Sonar Equation
SPL	Sound Pressure Level (L_p) in hydroacoustics
SSP	Sound Speed Profile (vertical)
TS	Target Strength (dB) in Sonar Equation

List of Symbols

A	Wave attenuation $A=20\log_{10}(e)\beta$ (dB/m)
a	Bubble radius (mm)
b	Damping constant in the Commander-Prosperetti dispersion relation
C_D	Drag coefficient
c	Sound speed in water (m/s)
D	Thermal diffusivity (m^2/s)
j	Imaginary unit $j=\sqrt{-1}$
K_m	Coefficient of eddy viscosity (m^2/s)
k	Wave number
L	Displacement in the dipole moment
$L_a(\omega)$	Acoustical skin depth (m)
$n(a)$	Bubble density as a function of bubble radius
S	Sound spectrum level in dB//μPa/√Hz
T	Wind stress (N/m^2)
u	Wind speed (m/s)
u_{10}	Wind speed at a height of 10 m
v	Particle velocity in a medium (m/s)
Z	Characteristic (acoustic) impedance of a medium (Pa·s/m =rayl)
β	Absorption coefficient (nepers/m)
γ	The ratio of specific heats
δ	Damping constant in bubble oscillation
ε	Fractional amplitude of bubble oscillation
κ	von Kármán constant
μ	Kinematic viscosity (Ns/m^2)
ρ	Density of a medium (kg/m^3)
ω	Angular frequency (1/s)

1 Introduction

Major applications of acoustics in developed societies are related to music and speech, as well as to noise reduction in industry and transportation. An important but less spectacular aspect of acoustic research is the use of sound and ultra sound technology in diverse branches of life and earth sciences. Typical applications in medicine include biomedical imaging and the effects of environmental noise on hearing, where acoustical engineering is a key technology providing vital information for physicians. High-resolution acoustic imaging of the seabed and more extensive seafloor mapping are the primary applications of underwater acoustics in marine geophysics. In order to illustrate the science of acoustics as a wide-ranging discipline, a compilation of current applications is presented in Fig. 1.1 as a pie chart [1].

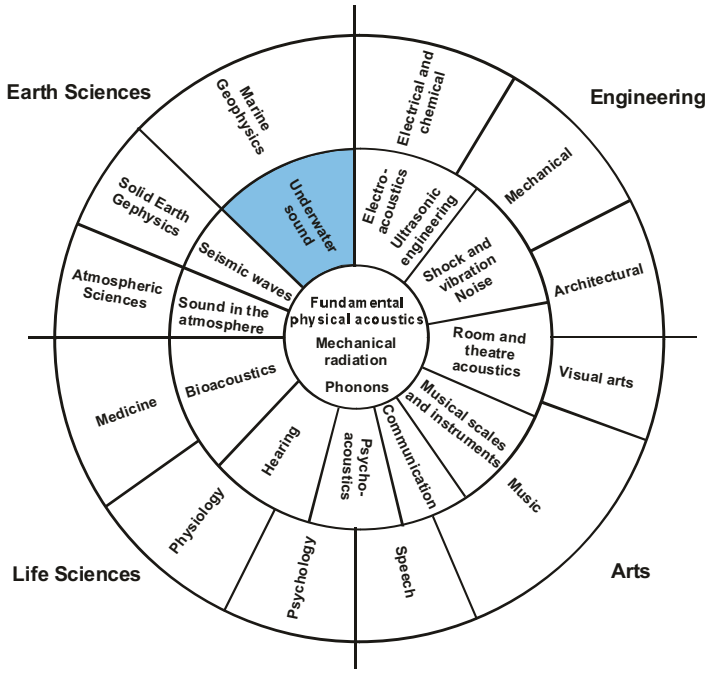

Fig. 1.1: The science of acoustics (adapted from Lindsay [1]).

Underwater acoustics represents a mixed discipline sharing aspects of physical acoustics, geophysics, and signal processing. It can also be considered as a branch of environmental acoustics if the focus is on underwater

noise and its effects on marine life. Developments in the field of underwater acoustics have been closely related to the requirements of naval forces, where antisubmarine warfare has been the main impetus for research. Dissemination of results has accordingly been hampered by the fact that most of the relevant research papers and reports are classified. The first edition of the widely known text book on underwater acoustics by Robert Urick was published in 1967 under the title “Principles of Underwater Sound for Engineers” [2].

Underwater ambient noise is a major environmental parameter in designing underwater detection and communication systems. Probability of detection of an underwater passive sound source or an active sonar target is a function of the underwater signal-to-noise (S/N) ratio [3]. Man-made underwater ambient noise in the oceans is mainly generated by shipping, where propeller cavitation is the most important source of underwater noise [4]. Ross has reported that low frequency ambient noise levels have increased by about 10 dB in the 25 year period since the early 1960s, and he estimated that the increase over the next quarter century would be about 5 dB [4]. Increasing ocean noise pollution has led to growing concerns about the effects of man-made noise on marine mammals [5]. This in turn has launched intergovernmental actions on establishing regulations to control oceanic noise pollution and to mitigate its effects on marine life [6]. In 2008 the members of the European Union signed the Marine Strategy Framework Directive (MSFD), which states in its qualitative descriptor no. 11 as follows: “Introduction of energy, including underwater noise, is at levels that do not adversely affect the marine environment”.

Major natural contributors to underwater ambient noise are breaking waves where oscillating bubbles and bubble clouds emit sound at lower frequencies, and combinations of bubble, spray, splash, and turbulence dominate sound sources at higher frequencies [P III]. Most studies on wind-driven underwater ambient noise are based on measurements carried out in deep ocean environments, where water salinities are typically seven times higher than those in the Gulf of Finland. The term “shallow” is historically defined as water less than 100 fathoms (600 ft ≈ 183 m) in depth, which is in the metric system usually rounded up to 200 m. A persistent problem in oceanic studies, however, is the difficulty in acquiring ambient noise data below 500 Hz without the dominating influence of shipping noise.

Ambient noise, although it is most often considered a drawback limiting system performance, contains information from which certain environmental parameters can be extracted. Passive bottom profiling and seabed imaging are enabled by cross-correlating vertically propagating ambient noise obtained from beamforming on a vertical hydrophone array [7].

The objective of the study was to identify major differences in characteristics of wind-driven underwater ambient noise between a shallow brackish water environment and the oceans. Underwater acoustics of the oceans is well documented in literature, but the existing knowledge of ambient noise in shallow brackish water is scarce. The Navy needs the information for underwater signal-to-noise ratio calculations in order to optimize sonar performance in all weather conditions. The present ambient noise data provides also a baseline for future man-made underwater noise studies by setting the limits of natural variation in ambient noise. Such studies are expected to grow in importance when the Marine Strategy Framework Directive is implemented within the European Union. This the reason why the overview contains a separate chapter on underwater hearing presenting thresholds levels for human ear and the variation of hearing thresholds among fish and marine mammals.

The present study deals with ambient noise measurements in shallow brackish water in an archipelago environment of the Gulf of Finland, conducted between August 2006 and March 2009. The measurement site is well shielded against low-frequency traffic noise from major sea lines. Characteristic features of the shallow, brackish water spectra are compared to those measured in oceanic areas using diverse spectral parameters fitted to ambient noise data. The high-frequency behavior of brackish water spectra is very likely controlled by both the bubble size distribution and the sound attenuation in a bubbly mixture under breaking waves. The relative importance of these physical processes in brackish water is modeled using established dispersion and noise models [P VI]. Prior to the brackish water calculations the bubble noise model is tested with oceanic bubble parameters. It establishes for the first time numerically the relation between the slope of -3/2 in oceanic bubble density and the high-frequency spectral slope of 5 - 6 dB/octave. The -3/2 bubble density slope was proposed in Nature in 2002 by Deane and Stokes [8]. They demonstrated the -3/2

power-law scaling for bubbles smaller than 1 mm in radius experimentally, and with the dimensional analysis of breaking wave jet entrainment.

The objectives set on the research were achieved, but interesting follow-up themes came up during the course of the study. Spatial variability of ambient noise in coastal areas is an important question, and the propagation of a broadband noise in a complex shallow water channel would be worth careful modeling. For the time being there has not been much open research in underwater acoustics in Finnish academic institutions due to a small number of civilian applications and the multidisciplinary nature of this branch of acoustics. The present study is presumably the first academic dissertation in Finland on underwater acoustics. Therefore a brief history of underwater sound and a restatement of some important acoustic equations and parameters are presented prior to the review of underwater ambient noise studies in oceanic areas and in the Baltic Sea.

2 Brief history of underwater sound

If you cause your ship to stop and place the head of a long tube in the water and place the outer extremity to your ear, you will hear ships at a great distance from you.

Leonardo da Vinci, 1490

2.1 General development

Perhaps the first scientific attempt to measure the speed of sound in water was the experiment in Lake Geneva in 1826 by the Swiss physicist Charles Sturm and French mathematician Daniel Colladon. They conducted a set of measurements to determine the travel time of the sound from a submerged bell to an underwater listening horn located at a distance of 13-14 km from the transmitting boat. The stroke of the bell was signaled to the receiving boat by a flash of light from burning powder [1]. Their experimental result for the speed of sound in water at 8 °C was c=1435 m/s, which is surprisingly close to the value of 1439 m/s obtained from today's approximate formulae for the corresponding conditions.

Until the outbreak of World War I underwater acoustics was almost entirely used as a navigational aid. Underwater bells were used in U.S. lighthouses and lightships as a sound source to signal their bearings to the ships equipped with the receiving system consisting of two “hydrophones”, i.e. two carbon-button microphones in a waterproof case. The system was used in conditions of bad visibility to replace lighthouse sirens, horns and whistles, whose sounds were easily masked by wind noise. In 1913 the pneumatically driven underwater bell was replaced by a more advanced underwater sound source developed by Reginald Fessenden. His electrodynamic transducer was able to transmit Morse code signals up to a distance of 50 km [9]. Underwater direction finding to lighthouses and lightships, however, was soon replaced by rapidly developing radio technology.

Shortly after the Titanic tragedy in 1912, Lewis Richardson filed patent applications in Britain for echo ranging with both airborne and underwater sound. Meanwhile in the U.S., Fessenden applied his transducer technology to echo ranging, and by 1914 he was able to detect an iceberg at a distance of about 3 km. The first experiments on depth sounding were carried out by a French research group led by Paul Langevin. Using an electrostatic transducer the group received echoes from the sea bottom in 1916. A year later in 1917, Langevin applied the piezoelectric effect to his new transducer which had a quartz-steel sandwich structure [2]. At the end of World War I, however, the echo ranging technology was not yet ready for operational use to counter the German submarine threat to the Allies. Instead, U.S. ships and submarines were equipped with a simple listening device, known as the SC tube, which was a mechanically rotated rubber bulb stethoscope. The two rubber detectors were spaced about 1.5 m apart, and they were connected to a stethoscope-like binaural headset by means of air tubes [10]. Parallel secret research work on transducer technology in Britain, led by Robert Boyle with Albert Wood, produced the first practical active sound detection equipment called ASDIC, which used the Langevin quartz apparatus as a transducer [9,11].

Between the two world wars the development of underwater acoustics was mainly focused on military applications, although the first echo sounders for ships became commercially available in 1925 both in the U.S. and in Great Britain. Quartz as a piezoelectric material was superseded by a synthetic Rochelle salt crystal and a magnetostrictive nickel tube structure [9]. The first Rochelle salt crystal hydrophones replaced obsolete carbon-button

microphones in American echo ranging equipment in the late 1920s [12]. Passive listening was soon abandoned in the U.S., and instead, the development was focused on high-frequency active sound detection, because it provided sharper beam patterns and therefore better bearing accuracy. In Germany, however, passive listening was still preferred, due to the lower attenuation of sound waves at audio frequencies, and due to the fact that the bulk of sound energy generated by ships is concentrated within the same frequency range.

Scientific knowledge of underwater acoustics made substantial progress in the period leading up to World War II. In the early 1930s the influence of bubbles on underwater sound was explained by Minnaert [13], who determined the resonance frequency of an air bubble radiating sound as a monopole source. The importance of a vertical temperature profile in refracting sound waves became understood as modeling of sound propagation in the sea made further progress. The first bathythermographs (BT) were constructed in the late 1930s, and by the outbreak of Word War II, every U.S. Navy ASW (Anti Submarine Warfare) vessel was equipped with the BT device [2].

A hydrophone array for passive listening in submarines and surface ships had also been developed by Germany. This GHG (Gruppenhorchgerät) group listening apparatus was the main underwater detection system used by the German Navy during World War II. The Allies gained possession of the system specifications after the capture of U-570 by the British in the summer of 1941. The GHC system had two 24 Rochelle Salt Crystal hydrophone arrays on either side of the boat. The hydrophone signals from preamplifiers were fed to an analog compensator and delay line circuitry to obtain acoustic beamforming to the bearing selected by the operator. The upper cutoff frequency of the audio bandwidth in the output to the headphones was 20 kHz, and the lower cutoff frequency was adjustable between 200 and 10.000 Hz [12,14]. The outstanding performance of the GHC prompted the Allies to try harder to bridge the capability gap in passive detection, but it was not until 1944, when the active sonar used by the U.S. Navy was augmented by the JP passive listening array [12].

Systematic studies on ambient noise in oceanic waters began in the 1940s. The high sonic band (20-50 000 Hz) in particular was extensively studied during the war by a group led by Vern Knudsen. The ambient noise results

of the wartime studies were summarized and published in a series of straight lines on a logarithmic scale ranging from 100 Hz to 20 kHz, known afterwards as the “Knudsen curves” [15].

After World War II civilian applications of underwater acoustics began to develop in parallel with military developments. Acoustic imaging of the seabed became possible with the emergence of sidescan sonars in the early 1960s, and multibeam echo sounders in 1970s. Echo sounding applications extended to the fishing industry for detection and localization of fish shoals, and to marine geology, where acoustic sediment (or sub-bottom) profilers were developed for seabed surveys. Underwater acoustic communication links and positioning systems are intensively utilized in today’s maritime industries and other offshore activities. Acoustic Doppler systems have been standard tools in physical oceanography since the late 1980s for measuring vertical current profiles from the bottom to the surface [16].

Concerns about the effects of man-made underwater noise on marine mammals emerged in the U.S. in the late 1970s after the studies on the disturbance reactions of arctic marine mammals to noise emissions related to oil and gas field developments [5]. The effects of low frequency active sonars (LFAS) on marine mammals have been studied since the mid-1990s when the first mass strandings of whales were reported and associated with the use of military sonar [17]. Underwater applications related to sound production, auditory capabilities, and communications of marine animals have formed a new multidisciplinary field of science called marine bioacoustics [18].

2.2 Early activities in the Gulf of Finland

The first documented underwater acoustic measurements in the Gulf of Finland were conducted during World War II for underwater surveillance. A coastal surveillance variant of the GHC apparatus manufactured by Atlas-Werke (Unterwasserschall-Gruppenhorchanlagen für Kustenhorchstationen) was installed at three locations in the central and eastern parts of the Gulf of Finland, on the islands of Kallbådan (Porkkala), Gogland (Suursaari), and Vaindlo [14,19,20]. The surveillance system had two circular arrays with 10 hydrophones in each array. The sensor units were deployed on the seabed about 8 - 12 km off shore, and the spacing between the arrays

was 3 - 6 km [14]. A block diagram of the coastal surveillance system is shown in Fig. 2.1.

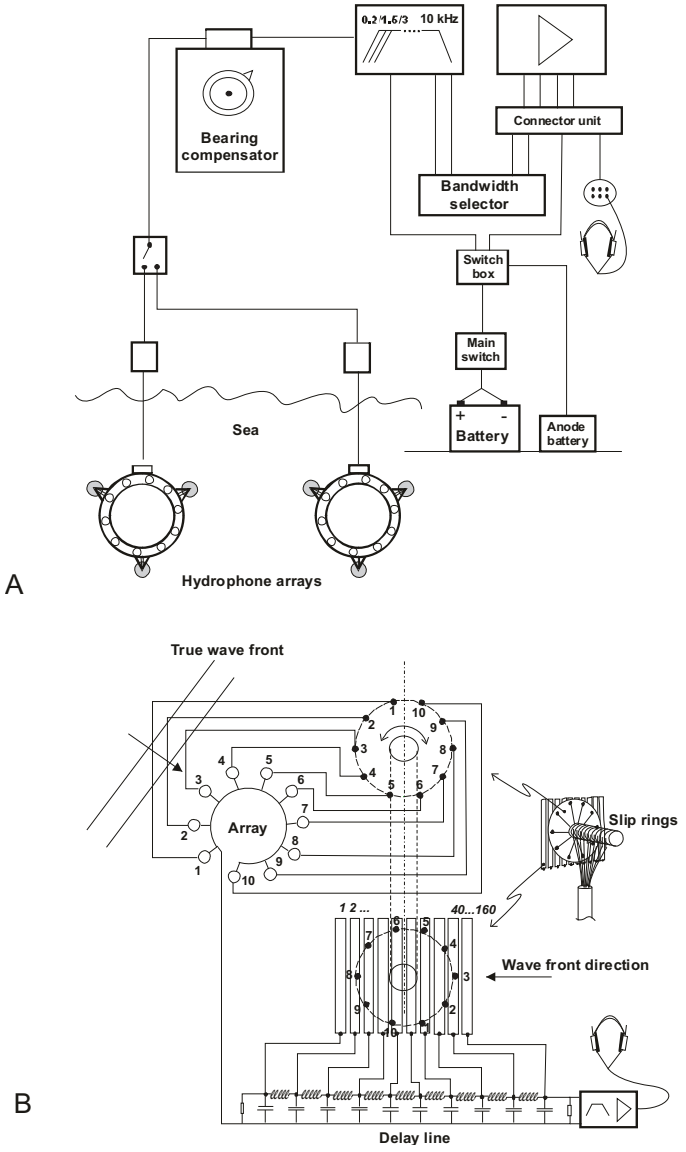

Fig. 2.1: Coastal underwater surveillance system (Unterwasserschall-Gruppenhorchanlagen für Küstenhorchstationen) by Atlas-Werke (1940) used in the Gulf of Finland during WWII. a) Block diagram of the system. b) Detailed structure of the analog bearing compensator unit performing analog beamforming (adapted from Knaapi [14]).

The analog beamforming in the receiver was performed by a mechanical strip-line compensator, which delayed the individual hydrophone signals by time lags corresponding to the sound wave front propagating from a selected bearing. The tapped analog delay line was accomplished as the ladder of LC low-pass π filters, where the delay of a single section was normally 17 μs, corresponding to approximately 2.5 cm of sound travel in water [12]. The number of strips in the compensator was typically 100, but it varied from 40 to 160 during the system's manufacturing history [21]. The sum of delayed hydrophone signals was bandpass filtered and fed to the headphones, see Fig. 2.1. The bandpass response was obtained with the cascade of high-pass and low-pass filters. The upper cutoff frequency was fixed at 10 kHz, and the lower cutoff frequency could be selected to 200, 1500, or 3000 Hz. [14].

3 Water as an acoustic medium

3.1 Sound waves in water

This section reviews some basic concepts in acoustics and compares their use and notation in air and underwater acoustics communities. Sound levels in acoustics are generally expressed as 10 times the logarithm of the square of the ratio of the sound pressure (p) to a reference pressure (p_{ref}), defining the sound pressure level (SPL or L_p) as [22]

$$SPL = 10 \log_{10} (p/p_{ref})^2 = 20 \log_{10} (p/p_{ref}) \quad (1)$$

The reference pressure in underwater acoustics is 1 μPa instead of 20 μPa used in air acoustics. The relation between intensity and effective pressure p (rms) for a plane wave in a physical medium i is defined as

$$I = p^2/\rho_i c_i = p^2/Z_i \,, \quad (2)$$

where ρ_i is the density, and c_i is the sound speed. The product $\rho_i c_i$ is the characteristic impedance Z_i , which is a medium dependent parameter. In the case of a plane wave Z is the ratio of acoustic pressure to the associated particle velocity v of a medium, according to "acoustic Ohm's law" $p = Zv$. Eq. (2) is valid also for spherical waves provided that the intensity is de-

fined as a real valued quantity. The sound intensity level (*IL*) is defined as 10 times the logarithm of the ratio of the sound intensity (*I*) to a reference intensity (I_{ref}), i.e.

$$IL = 10 \log_{10} (I/I_{ref}) , \qquad (3)$$

where the reference intensity now depends on the medium, unlike the reference value in the sound pressure level *SPL*. All relevant physical parameters and reference values for air and water are summarized in Table 1.

Water is a "high-impedance" environment, where pressures need to be multiplied by a factor of Z_{water}/Z_{air} in order to produce the same particle velocity as in air. The behavior of acoustical quantities in different media is outlined in Fig. 3.1 in terms of electronic circuit analogy. In an ideal "acoustic transformer" mechanical energy (intensity) is conserved in a lossless transfer from "primary" environment to the "secondary" one. If sound energy of a plane wave normally incident on the interface is equal in both media the pressure level and the particle velocity follow the ideal transformer equations, where $V = p$, $I = v$, and $N = \sqrt{Z}$, see Fig. 3.1. The pressure ratio between water and air $p_{water}/p_{air}=\sqrt{(Z_{water}/Z_{air})} \approx 60$ (35.5 dB). The pressure levels of equal sound intensity for air (L_p) and water (*SPL*) differ by 62 dB due to the difference (26 dB) in reference pressures; L_p = 0 dB re 20 µPa in air corresponds to *SPL* = 62 dB re 1 µPa in water. The difference of 62 dB is also obtained directly from the ratio of the reference intensities in Table 1.

Table 1: Physical and acoustical parameters for air and water [22].

Parameter	**Air**	**Water**	**Comment**
Density ρ (kg/m^3) @ 20˚C	1.21	998	Dist. water, 1 atm
Sound speed c (m/s) @ 20˚C	343	1482	Dist. water, 1 atm
Characteristic impedance Z (Pa·s/m)	415	$1.48 \cdot 10^6$	
Reference pressure p_{ref} (µPa)	20	1	
Reference intensity I_{ref} (W/m^2)	10^{-12}	$6.8 \cdot 10^{-19}$	

The atmosphere and the sea have also different sound absorption properties, absorption in the sea being substantially lower than in the atmosphere at audio frequencies. Absorption coefficients for sound at 1 kHz in diverse sea areas lie within the range 0.03 - 0.09 dB/km at 4˚C [P I], while standard absorption coefficients (ISO 9613-1) for air at 1 kHz and at 10 ˚C are

in the range 3.5 – 5.1 dB/km for relative humidities greater or equal than 40 %. The atmosphere is a hemispherical space in which the sound from a confined 3-dimensional source propagates more or less as a spherical wave which has a geometrical spreading loss of 6 dB per doubling of distance. However, traffic noise from highways is modeled as a line source having a spreading loss of 3 dB/oct in distance. Besides, atmospheric stratification and wind may create conditions where propagation loss is less than predicted by the elementary theory.

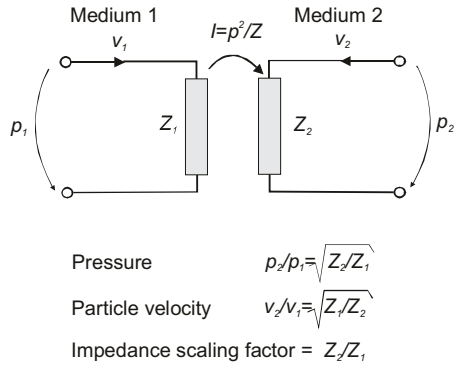

Fig. 3.1: Normally incident plane wave at a boundary of two media presented in terms of ideal acoustic transformer.

In shallow water underwater sound propagates in a waveguide bounded by the sea bottom and the surface, with the latter acting as a pressure release boundary with a high impedance mismatch. Under these conditions sound waves typically spread in a cylindrical manner with a spreading loss of 3 dB/oct in distance. Real propagation conditions are however governed by a vertical sound speed (temperature) profile which can create various forms of ducted propagation with complex loss patterns [23]. These characteristics of underwater sound propagation largely explain why the sound from a merchant ship is under favorable conditions audible over distances of up to a few tens of kilometers.

3.2 On underwater hearing

Underwater environment changes sound transmission properties in the human auditory system compared to those prevailing in normal listening conditions in air. The outer ear and the auditory canal are filled with water having the sound speed 4.4 times higher than that in air. Sound

transmission from the ear canal through the eardrum up to the liquid filled cochlea is affected by several medium boundaries where the characteristic impedance changes. Somewhat surprisingly however, it has been found that the presence or absence of an air bubble in the ear canal has no significant effect on underwater hearing thresholds [24]. In water, sound waves reach the cochlea without a significant loss of energy, because a human head is acoustically more transparent in water than in air, due to good impedance match between water and the head. It has been reported in many studies [25,26] that underwater sound above 1 kHz is detected predominantly by bone conduction rather than ear canal (tympanic) conduction, while in air, bone-conducted thresholds are about 60 dB higher than those of ear conduction [27]. Localization abilities in water, however, have been found to degrade significantly if ear conduction is technically blocked off [25,28].

Underwater hearing thresholds for human ear, fish, and marine mammals are compiled in Fig. 3.2. The thresholds are presented as the intensity level, which is a medium-independent measure of the rate of energy flow to an auditory system. The reference intensity level in all data sets is 10^{-12} W/m^2. The use of the equalized intensity scale enables better comparison of sound levels measured in air or water, as demonstrated by Dahl *et al.*[31]. In terms of the equalized intensity the human hearing thresholds in air and water seem to be virtually identical at frequencies below 1 kHz, while at higher frequencies the underwater threshold are substantially higher. The difference between the air and the underwater thresholds above 1 kHz is most likely attributable to the increasing dominance of bone conduction in water at higher frequencies [25,26].

For the sake of comparison, typical hearing thresholds for fish and marine mammals are depicted together with the human thresholds. Fish lack both the outer and the middle ear, as well as the cochlea. The inner ear consists of semicircular canals and the otolithic organs, which are typically located within the skull behind the eyes [18]. The hearing sensitivity of a fish species is enhanced if its swim bladder and the inner ear have a structural connection. This connection can be mechanical, through the Weberian ossicles (e.g. carp), or else the swim bladder directly enters the skull (e.g. herring). Fish are also able to sense low-frequency vibrations through the lateral line system, which helps the fish in collision avoidance, self-orientation, and prey location [30].

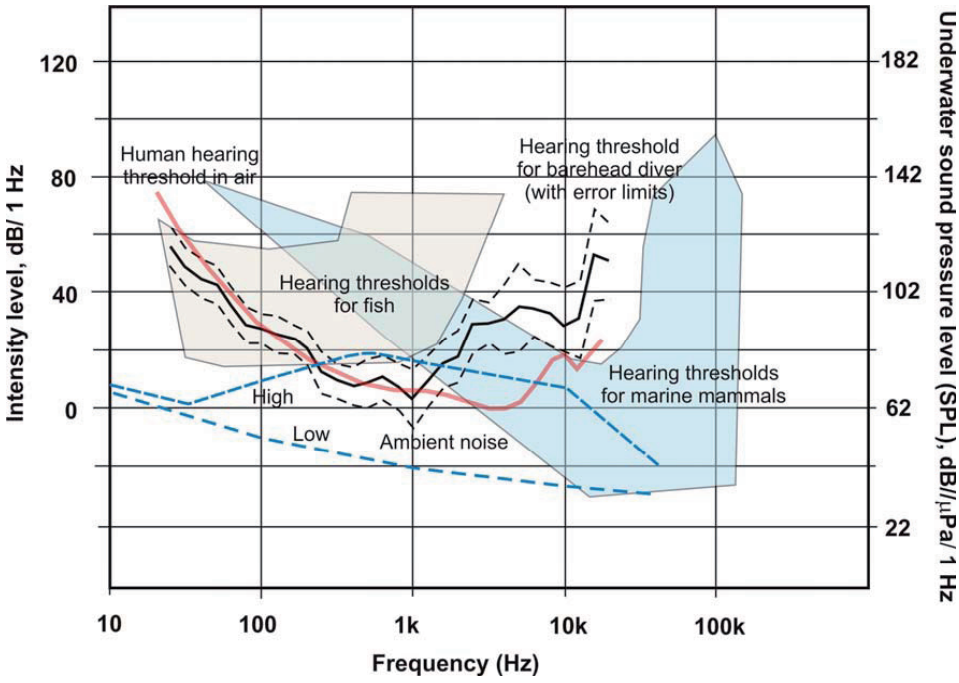

Fig. 3.2: Human hearing thresholds in air (red) [22] and in water (black) [29] compared to those of fish and marine mammals (adapted from [18,29,30]). High and low underwater ambient noise levels represent shallow brackish water [P V].

Marine mammals have the cochlea in their inner ear but external ears are typically absent. Channeling of sound to the middle ear also differs substantially from that of land mammals [30]. Hearing frequency bands for marine mammals extend above 100 kHz, and are therefore about two orders of magnitude higher than those of fish. The high and low underwater ambient noise levels obtained from this study [P V] are depicted in the same figure as power spectral densities.

4 Wind-driven underwater ambient noise

4.1 Wind characteristics above the air-sea boundary

Wind is the key physical factor generating waves at sea. Wind speed above the sea surface is not uniform, but it varies as function of altitude within the atmospheric (planetary) boundary layer (ABL). It is the interaction zone

between the free atmosphere and the sea surface, where exchange of heat and momentum occurs between sea and air causing turbulence in air flow. The depth of the atmospheric boundary layer varies from few tens of meters above cold Arctic seas to 1 - 2 km above warm tropical seas. The lowest tenth of the ABL, in contact with the sea surface, is called the surface layer, where turbulent mixing is intense [32].

The mechanical interaction that transfers momentum from air to sea is the wind stress T (N/m²), which is proportional to the square of the wind speed u as $T = \rho_a C_D u^2_{10}$, where ρ_a is the density of air, C_D is the dimensionless drag coefficient, and u_{10} is the wind speed at 10 meters. An alternative quantity for the wind stress is the friction velocity $u^* = \sqrt{(T/\rho_a)}$. The drag coefficient may now be determined as the square of the ratio of two velocities, i.e. $C_D = (u^*/ u_{10})^2$. The drag coefficients determined from u_{10} range typically from 0.0005 to 0.0025 as wind speed increases from 3 to 25 m/s [32,33,34].

An approximate solution for wind speed above the sea surface is obtained from the turbulent boundary layer theory applied to a smooth surface. Turbulent air can be treated as a viscous medium where the coefficient of eddy viscosity K_m is defined as the ratio of u^{*2} and the velocity shear (velocity gradient $\partial u/\partial z$). The eddy viscosity increases linearly with height (z) due to growing size of air eddies. Theodore von Kármán formulated this in functional form as $K_m = \kappa u^* z$, where κ is the von Kármán constant (κ=0.4 for airflow over the sea surface). Substitution of this relation to the definition of the eddy viscosity leads to a simple first-order differential equation $\partial u/\partial z = u^*/\kappa z$. Setting velocity to zero at the boundary surface, $u(z_o)$=0, the wind speed profile is solved as

$$u(z) = (u^*/\kappa)\ln(z/z_o) , \qquad (4)$$

where z_o is the roughness length of the sea surface. It is obtained from Charnock's relation $z_o = 0.0156\ u^{*2}/g$, where g is the gravitational acceleration [32].

All the wind speed measurements reported in this study are made at a standard measurement height of 10 m using Vaisala WXT weather transmitter station installed in the test site [P V]. Wind speeds in the study are the average values over the time periods of sound recordings. Unstable

and gusty wind conditions were avoided, but the measurements were mostly conducted in steady winds where sea state conditions in the confined test site were fully developed.

4.2 Oceanic and laboratory studies on noise mechanisms

The wind speed dependence of ambient noise in the wartime Knudsen curves has proved to be valid and useful at frequencies greater than 1 kHz. At lower frequencies, however, wind noise processes are more complex and shipping noise may be considerable and difficult to distinguish from wind-driven noise. A comprehensive review of the early oceanic studies was given by Wenz [35]. Sources of ambient noise proposed in diverse oceanic studies prior to the early 1980s were discussed by Urick [36], and the results were summarized as a conceptual view of noise spectra over the frequency range from 1 Hz to 100 kHz.. Wind noise generation processes are different at high and low frequencies, and there is a flat region between them. Wenz proposed that turbulent-pressure fluctuations could be the physical mechanism behind the low frequency behavior, while bubbles and spray resulting from surface agitation are the sources of wind noise at higher frequencies. The latter assumption was partially based on the laboratory experiments carried out by Franz in the late 1950s, in which two distinct noise mechanisms for underwater sound were identified, namely the impact of a water drop on the surface and bubble volume pulsations [37]. Oceanic underwater ambient noise curves originally compiled by Wenz are depicted in Fig. 4.1.

Shipping noise dominates the ambient noise spectrum at frequencies from 20 to 200 Hz. Wenz classified shipping noise into two types. *Ship noise* is the short-term noise component from one or more ships passing the hydrophone at close range. It is usually obvious and therefore easy to remove from ambient noise data. *Traffic noise* is the cumulative effect of all distant shipping in the surrounding sea area. It generates a stationary maximum in ambient noise spectra, which easily masks the noise from other sources.

Noise from the thermal excitation of the medium itself begins to dominate the wind-driven noise at frequencies from 50 to 200 kHz depending on sea state. Mellen derived an expression for underwater thermal noise using classical statistical mechanics. The energy from compressional normal modes of thermal vibration in a unit volume is determined as function of

frequency. The higher the frequency, the more normal modes, i.e. degrees of freedom of the system, are included in the volume. The final expression is equivalent to the Rayleigh-Jeans law for blackbody radiation, where the spectral radiance of electromagnetic radiation increases with increasing frequency [38]. Mellen's expression for the thermal noise (molecular agitation) is depicted in Fig. 4.1 together with the extrapolated Knudsen (Wenz) curves.

Research activity into natural mechanisms and physical sources of ambient noise increased in the 1980s and breaking waves became the subject of intensive study [40]. A comprehensive review on low-frequency ambient noise was given by Carey and Browning [41]. By the early 1990s it was generally recognized that the major contributors to low-frequency underwater ambient noise are oscillating bubbles and bubble clouds generated by breaking waves. At higher frequencies combinations of bubble, spray, splash, and turbulence caused by breaking waves are the primary sources of sound [42,43,44]. A persistent problem in the low-frequency studies, however, is the difficulty in acquiring ambient noise data below 500 Hz without the dominating influence of traffic noise.

It is well established that bubble size distribution in sea water is controlled by salinity although experimental results are quite variable depending on the method used. The effect of salinity on ambient noise caused by breaking waves was simulated with a tipping trough experiment by Carey *et al.* [45], who showed that salinity controls bubble size distribution such that the proportion of small bubbles increases markedly with increasing salinity. This phenomenon was seen as higher ambient noise levels above 4 kHz. The level of acoustic radiation was also found to depend on salinity.

In another laboratory experiment, breaking waves were simulated in a wave tank, where the bubble size spectra were found to be ten times higher in oceanic-like saltwater than in fresh tap water [46]. Other studies on the effect of salinity on bubble size distribution have been reported by Winkel *et al.* [47], Kolaini [48], and Orris and Nicholas [49]. A common trend in all the experiments is, however, the tendency of a bubble to grow in size as salinity decreases. This is because freshwater bubbles coalesce easily, whereas saltwater bubbles repel each other due to their different surficial physico-chemical properties [46].

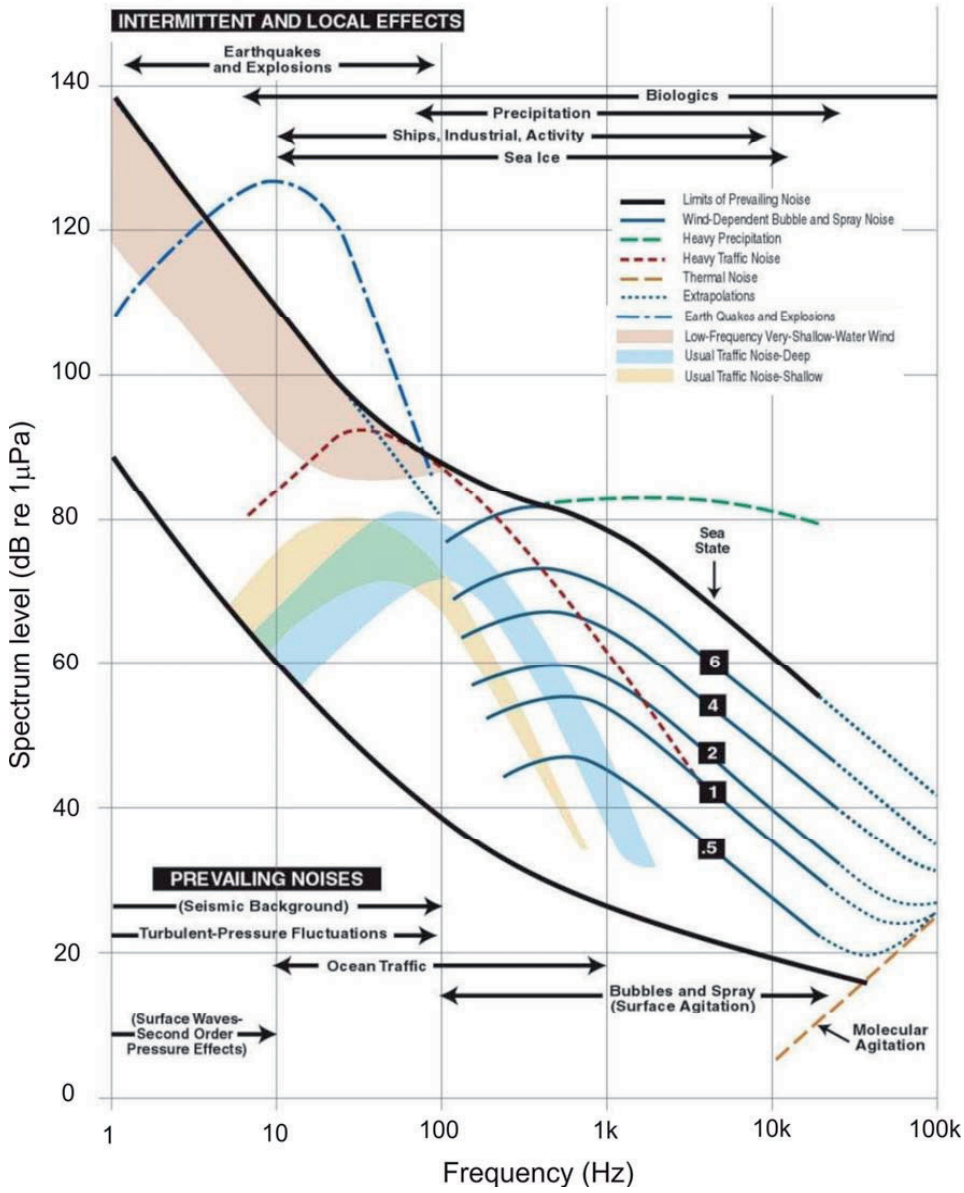

Fig. 4.1: Underwater ambient noise in oceanic environment. Redrawn from Wenz [35] and OSB/NRC [39].

Deane and Stokes [8] measured bubble size distributions inside breaking waves in the laboratory and in the open ocean. They were able to demonstrate two distinct physical mechanisms controlling bubble size distribution. Bubbles less than about 1 mm in radius exhibit a bubble size distribution proportional to $a^{-(3/2)}$ as a result of jet and drop impact on the wave face. Bubbles larger than about 1 mm are subject to fragmentation by turbulent and sheared flow, and therefore exhibit steeper power law scaling $a^{-(10/3)}$. Surface tension has an important influence on these mechanisms, and is controlled both by the salinity and also by the amount of various chemical agents or impurities in sea water. It has been reported that the surface tension values of bubbles in "clean" fresh water can be twice as great as those in "dirty" ocean water. It is evident that bubbles in brackish water have higher surface tension than those in the ocean, thus leading to differences in bubble size distributions [49,50].

5 Measurements in the Baltic Sea area

The Baltic Sea is a confined shallow water basin where the salinity of water is substantially lower than the typical value of 35 ppt in the oceans. The maximum depth in the Baltic Sea is 459 m, the average depth being around 65 m. The corresponding water depths for the Gulf of Finland are 123 m and 38 m, respectively. Salinities in the Baltic Sea vary from 6 to 9 ppt, and in the Gulf Finland it decreases from 6 ppt in the west to 3 ppt in the east [51]. The physical environment of the Gulf of Finland including bathymetric features and seasonal sound speed profiles are discussed in more detail in [P I]. A map of the Baltic Sea and the locations of the ambient noise measurements referred in this study are compiled in Fig. 5.1.

Wille and Geyer [52] reported measurements relating to a study of the variability of wind-dependent ambient noise in the North Sea and the Baltic Sea. They concluded that wind stress caused by the wind speed at the sea surface governs the noise production, the role of sea wave height being secondary. Seasonal variations observed in the dependence of ambient noise level on wind speed at anemometer height were explained by a variation in atmospheric stratification caused by a temperature difference between air and water. The influence of propagation loss on wind-dependent ambient

noise in shallow water appeared to be marginal. Wagstaff and Newcomb [53] reported seasonal variations of about 12 dB in ambient noise levels obtained from five sites in the southern Baltic Sea. The measurements were conducted at frequencies from 20 Hz to 2 kHz using calibrated sonobuoys. The elevated winter levels were explained by more intense shipping activity and commercial fishing, and by lower acoustic propagation losses in winter.

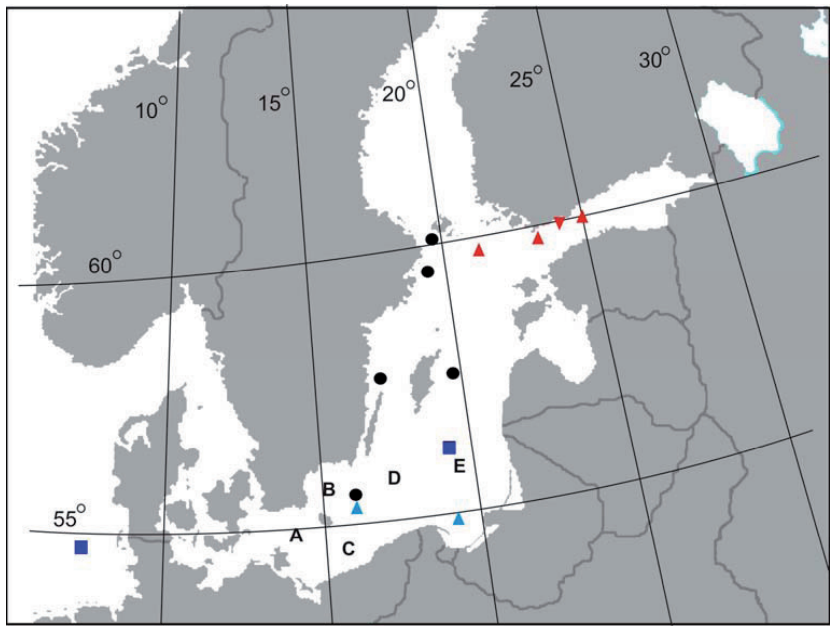

Fig. 5.1: Map of the Baltic Sea. locations of the reported ambient noise measurements: ■ Wille & Geyer [52], ▲ Poikonen & Madekivi [P I], ● Pihl *et al.* [55], **(A…E)** Wagstaff & Newcomb [53], ▲ Klusek & Lisimenka. [54], ▼ Poikonen & Madekivi [P III], Poikonen [P V].

Klusek and Lisimenka [54] performed ambient noise measurements in the Gdansk Gulf Deep in summer conditions, and in the Bornholm Deep in winter conditions. The data were collected at two depths using autonomic acoustic buoys. Seasonal variations were observed in ambient noise, which changed significantly as a function of depth, depending on the structure of a seasonal waveguide.

The Swedish Defence Research Agency (FOI) conducted ambient noise measurements in five locations in the Baltic Sea [55]. The results followed the standard curves by Wenz [35] except at frequencies below 100 Hz,

where the measured levels were lower. Subsequently, FOI reported wind-driven ambient noise measurements from a shallow water environment in the Stockholm archipelago. The ambient noise spectra developed a steep spectral decline below 500 Hz with increasing wind speed [56].

The Finnish Navy conducted a series of ambient noise measurements in the Gulf of Finland in the early 1990s. The data were collected with fixed bottom-mounted hydrophone systems located in three sites, see Fig. 5.1. Ambient noise samples of five minutes duration were recorded every four hours. The ambient noise levels at moderate winds appeared to be 5 - 10 dB lower in summer than in winter. A potential explanation for this is the higher proportion of cumulative noise in winter due to a flat seasonal temperature (i.e. sound speed) profile favouring long-range sound propagation [P I].

Poikonen and Madekivi [P III] reported the underwater ambient noise measurements in shallow (15-20 m) brackish water in the archipelago of the Gulf of Finland covering an entire one year period, based on measurements made between August, 2006 and August, 2007. The frequency range of the measurements was from 20 Hz to 10 kHz. Follow-up measurements were carried out a year later in the same area, where the frequency range was extended up to 70 kHz. The second data set also covered a complete year. Meteorological sensors were set up at 10 m above sea level on the top of the station to provide temperature, pressure and wind conditions during the measurements. A calibrated omnidirectional hydrophone (TC4032) was deployed in a tripod on the seabed.

The hydrophone has a flat frequency response (2.5 dB) from 10 Hz to 80 kHz and a sensitivity of -170 dB re V/μPa. The hydrophone signal was transferred to the shore in analog form. The calibrated analog signal from the preamplifier was sampled with a 16-bit resolution at a rate of 44.1 kHz in the first study, and at 176.4 kHz in the broadband measurements. The transmission bandwidth (3 dB) of the analog hydrophone cable is around 200 kHz, and the attenuation in the whole measuring band is less than 0.5 dB. The noise level of the hydrophone was sufficiently low for all the conditions where ambient noise was measured. Fig. 5.2 shows the hydrophone (system) noise level together with the extreme spectrum levels measured in the broadband study.

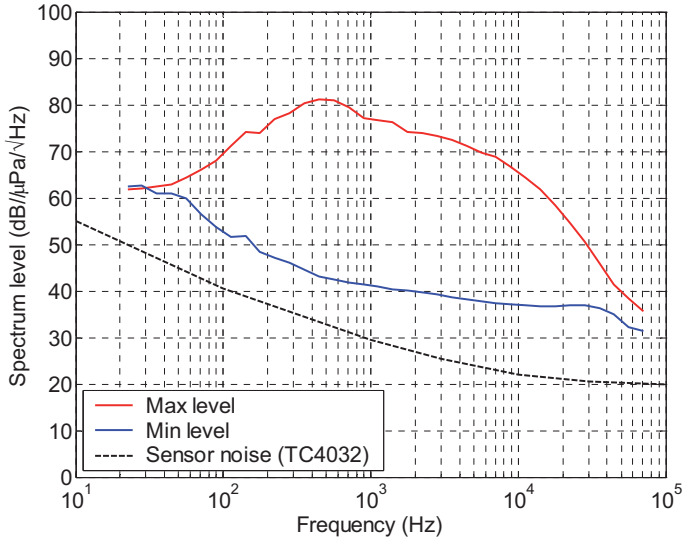

Fig. 5.2: Hydrophone (system) noise level together with the extreme spectrum levels measured in the broadband study [P V].

Smoothed power spectral density (PSD) estimates were obtained using the Bartlett's procedure, where individual periodograms are averaged over a number of independent samples. The variance of the Bartlett's estimate is inversely proportional to the number of periodograms averaged. The estimate is consistent because the variance approaches zero as the number of samples becomes large [57].

The procedure applies well to wind-driven noise signals because they are fairly stationary in time domain and their spectral structure is smooth. All the PSD estimates in the study were calculated as the average of 32 1-second samples. Interfering frequency lines, such as power harmonics, were removed from the spectra using the non-linear 9-point median filtering. Further smoothing was obtained by calculating total power for 1/3-octave bands and then normalizing the band power to a 1-Hz band [P II].

The effect of a sea bottom on underwater noise was estimated in [P III] using a physical noise model which calculates the acoustic intensity from the infinite acoustic dipole distribution at the sea surface. The intensity element of integration in the model, based on Eq.(4.36) in [16], is however incorrect. The only cumulative term in the integration is the vertical component of intensity. The horizontal components from the elementary di-

poles on the opposite sides of the annulus of integration point to opposite directions thus canceling each other out.

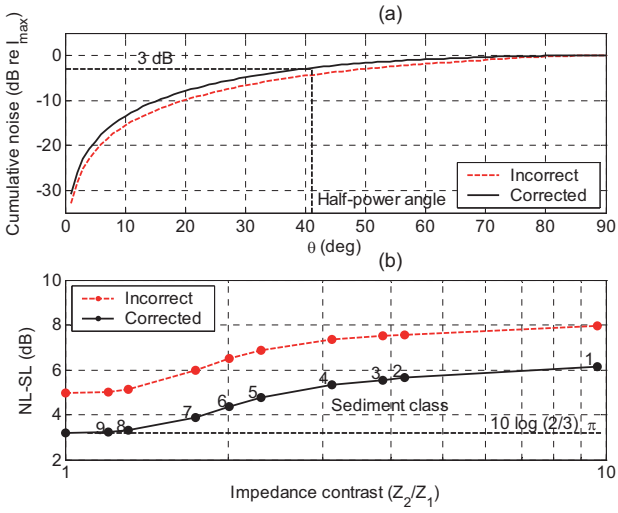

Fig. 5.3: (a) Corrected accumulation of noise intensity with increasing zenith angle (θ). (b) Corrected difference between noise level (NL) and source level (SL) versus impedance contrast Z_2/Z_1 for nine typical Baltic sediment classes which are Rock (1), Till (2), Till formation (3), Sand and gravel (4), Secondary sand (5), Glacial mixture (6), Silt and clay (7), Post glacial clay (8), and Recent mud (9). See Fig. 2 in [P III].

The correct expression for the total intensity is obtained by multiplying the direct intensity element by cosθ, and the bottom-reflected intensity element (Eq.(1) in [P III]) by cosφ before numerical integration. The correct relationship between noise level and source level in homogeneous deep water takes now the form $I_D \approx (2/3)\pi I_o$. The corrected results are depicted in Fig. 5.3. together with the inaccurate curves from [P III]. The cumulative noise curve in the upper panel becomes slightly steeper, so that the half-power value is now reached at an angle of 41° instead of 49° obtained in [P III]. The level of the intensity values in the lower panel is shifted down by 10log(2/3) ≈ 1.8 dB, but the impedance contrast dependence, i.e. the sea bottom effect, remains practically unchanged. Therefore the correction does not much change the major conclusions drawn from the erroneous curves.

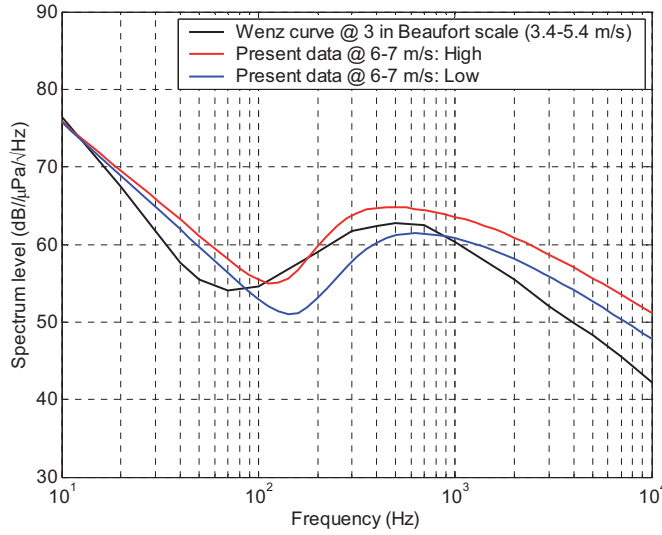

Fig. 5.4: Shallow water spectra of the present study compared to the estimated spectrum given by Wenz for the case with no traffic noise [35].

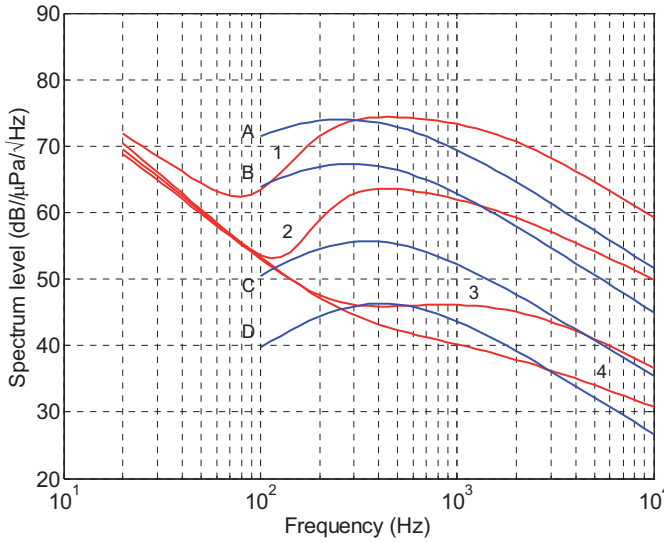

Fig 5.5: Shallow and brackish water ambient noise curves (red) compared to the average deep ocean curves (blue). Wind speeds for the curves are 14-16 m/s for A and 1, 6-8 m/s for B and 2, < 3 m/s for C and 3, and < 0.5 m/s for D and 4 [P III].

The shallow water curves of the present study were compared to the estimate given by Wenz for the case with no traffic noise, see Fig. 14 in [35]. The shapes of the curves are surprisingly close to one another, but the level of the present curves is slightly lower than that in Wenz's estimate. Wind speeds of 6 - 7 m/s (wind force 4 in Beaufort scale) in the present data are required to reach the level obtained at wind force 3 in the Wenz curve, Fig. 5.4.

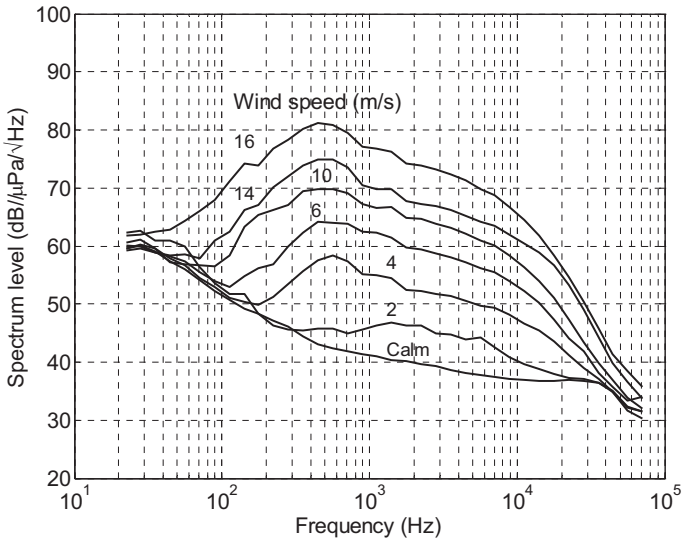

Fig. 5.6: Set of ambient noise curves in the broadband data set exhibiting steepening spectral slopes above 10 kHz at intermediate and high wind speeds [P V].

The ambient noise levels in the first study [P III] were fairly close to the average deep water levels for the highest wind speeds but the wind speed dependences differed markedly from one another, as shown in Fig. 5.5.

Ambient noise of the broadband data set [P V] exhibited a dual-slope spectral pattern at intermediate and high wind speeds, where high-frequency spectral slopes were substantially steeper than those at medium frequencies, see Fig. 5.6.

6 Parameterizing ambient noise spectra

6.1 General principles

The objective of using parametric models in the interpretation of spectral features is to reduce system complexity by relating model parameters to principal physical processes that are behind measured ambient noise. Typical filter parameters, such as half-power frequencies and spectral slope factors (roll-offs), applied to ambient noise spectra, are related to the structure of bubble size distribution in breaking waves. Low-pass filter parameters above 1 kHz are measures of the slope factors of a bubble size distribution [P VI]. The largest bubble size or the existence of bubble clouds can be estimated from high-pass filter parameters applied to low-frequency ambient noise spectra [P III].

In the first data set the curve fitting was mostly performed by a visual estimation where the parameters were manually adjusted to obtain the best fit [P III]. Although the visual fit performed well, a numerical curve fitting routine using a least squares solution was applied to the second data set [P IV-VI]. Uncertainty in fitting the model was estimated with a deviation calculated from the residual sum of squares (RSS). The quality of fit between measured and modeled spectra was generally high; residual deviations for the fitted curves were typically less than 1 dB.

6.2 Frequency responses

The characteristic features of measured ambient noise spectra are parameterized using a multi-parameter logarithmic model. The ambient noise spectrum level normalized to a 1-Hz band is approximated with a “frequency response” type filter curve fitted to the measurements. The noise model is made up of three segments of different type and slope. The seven-parameter expression for the noise power spectral density S (dB//μPA/√Hz) may be written as [P III]

$$S(f) = S_0 + 10\log\left\{\frac{\left[1+\left(\frac{f_0}{f}\right)^{m_0}\right]}{\left[1+\left(\frac{f}{f_1}\right)^{m_1}\right]\left[1+\left(\frac{f_2}{f}\right)^{m_2}\right]}\right\}, \qquad (5)$$

where S_o is constant spectral density level, f_o, f_1 and f_2 are the half-power (3 dB) frequencies of the model segments 0-2 (filter blocks) , and m_0, m_1 and m_2 are the spectral slope factors. A pure bandpass model is obtained using only the filter blocks 1 and 2.

The dual-slope pattern above 1 kHz in the broadband spectra is parameterized by means of a three-parameter logarithmic curve that fits two spectral slopes to measured data. The noise power spectral density takes now the form [P VI]

$$S(f) = S_0 - 10\log\left\{\left[1+\left(\frac{f}{f_1}\right)^{m_1}\right]\left[1+\left(\frac{f}{f_2}\right)^{m_2}\right]\right\}, \qquad (6)$$

where m_1 and m_2 are the spectral slope factors, and f_2 is the second half-power frequency at which the spectral slope steepens. S_o is the spectrum level parameter, and f_1 is the first half-power frequency that is outside the frequency band of interest.

6.3 Wind speed dependence

The wind speed dependence of ambient noise is estimated with the aid of a two-parameter logarithmic curve [P III]

$$S(u) = S_0 + 10\log\left[1+\left(\frac{u}{u_c}\right)^{\eta}\right], \qquad (7)$$

where S and S_o are noise power spectral densities (dB//μPA/√Hz), u is wind speed (m/s), u_c is the threshold wind speed, and η (=k in [P II-V]) is the wind speed dependency factor. The curve describes the wind speed de-

pendence in two wind speed regions separated by the threshold value of u_c. In the lower noise-limited region no wave breaking occurs and the ambient noise shows no dependency. In the higher region above the threshold wind speed, wave breaking starts and the ambient noise rises with increasing wind speed at a rate determined by the factor η. The model curve of Eq. (7) was fitted to the spectral data as a function frequency and the results are plotted in [P III and V]. Typical ranges for the threshold wind speed (u_c) and the wind speed dependency factor (η) are 2 - 10 m/s and 3 - 8, respectively [P III-V].

In [P III] the wind speed dependence curve has an additional term to model possible spectral saturation above a certain saturation wind speed u_s, where sea state conditions become fully developed and the noise level starts to saturate. In the published literature the wind speed dependence is often expressed by the relationship $S \sim u^{2n}$, originally introduced by Piggott [58]. The wind speed dependence factor η in Eq. (7) is then twice the value of Piggott's factor n, i.e. $n = \eta / 2$.

7 Modeling ambient noise

7.1 Bubble absorption

Underwater sound is modeled in terms of pressure fluctuations propagating as a plane wave. The propagation through a dispersive medium is governed by the complex wave number depending on angular frequency ω, i.e $k = k(\omega)$ [*]. In a one-dimensional (x) situation a traveling plane wave for pressure (p) may be written in complex form as

$$p = p_o e^{j(\omega t - kx)}, \tag{8}$$

where $j = \sqrt{-1}$. Setting $k = \alpha - j\beta$, the plane wave expression takes the form

$$p = p_o e^{-\beta x} e^{j(\omega t - \alpha x)}. \tag{9}$$

[*] The standard (SFS-EN ISO 80000-8) definition for the complex wave number is $k = \beta - j\alpha$. In hydroacoustic in general [16], and in bubble absorption studies in particular [59] the term β has been used also as an absorption coefficient.

The absorption coefficient β (nepers/m) determines the attenuation of a plane wave while the coefficient α controls its phase speed. The attenuation A in dB/m is obtained from β as $A = 20\log_{10}(e)\,\beta \approx 8.686\,\beta$. In electromagnetism the inverse of β is defined as the skin depth (δ) at which the wave amplitude decays to 1/e of its initial value. Deane [59] has adopted the same concept to hydroacoustics, defining the acoustical skin depth in a bubbly medium as $L_a(\omega) = 1/\beta(\omega)$. The complex wave number in a bubbly mixture with volume fractions up to 1 - 2% is obtained from the dispersion relation given by Commander and Prosperetti [60]

$$k_b^2 = \frac{\omega^2}{c^2} + 4\pi\omega^2 \int_0^\infty \frac{a\,n(a)\,da}{\omega_0^2 - \omega^2 + 2jb\omega}\ , \qquad (10)$$

where c is the speed of sound in pure sea water, a is the bubble radius, $n(a)$ is the bubble size distribution as a function of radius a, and ω_o is the natural angular frequency, see Eq.(13). The complex damping constant b is of the form

$$b = \frac{2\mu}{\rho a^2} + \frac{P_0}{2\rho a^2 \omega}\mathrm{Im}(\Phi) + \frac{\omega^2 a}{2c}\ , \qquad (11)$$

where μ is the kinematic viscosity, P_o is the undisturbed pressure in the bubble, ρ is the density of water. Φ is the complex function of the ratio of specific heats γ, the thermal diffusivity D, the angular frequency ω, and the bubble radius a [49].

A bubble size distribution curve used in the study [P IV and VI] for brackish water spectra is

$$n(a) = \frac{n_0}{\left[1 + \left(\frac{a_1}{a}\right)^{k_1}\right]\left[1 + \left(\frac{a}{a_2}\right)^{k_2}\right]}\ , \qquad (12)$$

where a_1 and a_2 are the lower and higher half-value limits ($n=½n_o$) of a bubble size distribution, and k_1 and k_2 are the corresponding power law dependencies on radius.

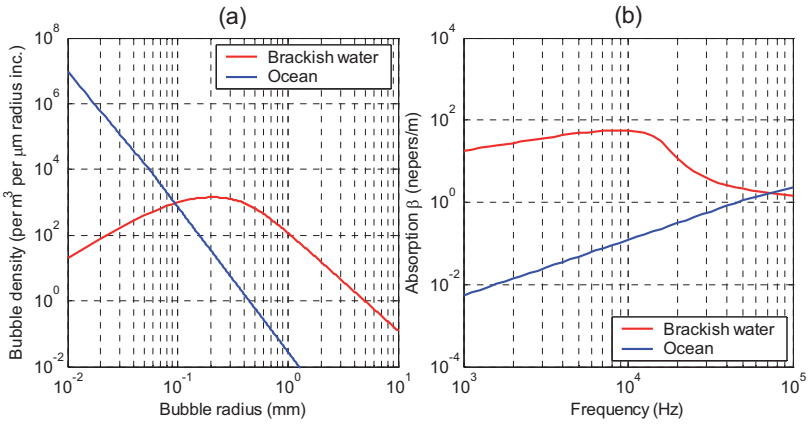

Fig. 7.1: (a) Bubble densities for oceanic (blue) and brackish water (red) environments, and (b) the corresponding absorption curves.

Absorption curves were calculated for bubble size distributions in diverse environments from fresh water to ocean, and the results are presented in [P VI]. The calculations demonstrate that absorption in brackish and fresh water, unlike in ocean water, tends to decrease above a frequency of 10 kHz due to the low proportion of small bubbles in a bubbly mixture created by breaking waves. Fig. 7.1 shows typical bubble size distributions for oceanic and brackish water environments [P VI]. The brackish water curve is according to Eq.(12) with the parameters a_1=0.1 mm, a_2=0.4 mm k_1= 2, and k_2= 3. The oceanic curve given by Medwin [61, p. 330] yields a rising trend in absorption as frequency increases. The absorption of the brackish water distribution, however, declines at higher frequencies due to the low proportion of small bubbles resonating above 10 kHz. This leads to the conclusion that the excess high-frequency attenuation in the brackish water spectra shown in Fig. 5.6 cannot be attributed to absorption in a bubbly mixture. Instead, the properties of the power spectrum caused by resonating bubbles provide the most probable explanation for the steeper slopes.

7.2 Resonating bubbles

It is well established that the primary source of ambient noise from less than 1 kHz up to around 50 kHz is the cumulative sound from individual bubbles oscillating at their linear resonant angular frequency [13,61]

$$\omega_i = \frac{1}{a_i}\sqrt{\frac{3\gamma p_0}{\rho}}\ , \tag{13}$$

where a_i is the radius of the bubble i, γ is the ratio of the specific heats of the bubble gas, p_o is the ambient bubble pressure, and ρ is the density of water. Loewen and Melville introduced a model for calculating the sound from a bubble size distribution where individual bubbles are oscillating at their lowest mode frequency and are sufficiently close to a pressure release surface to radiate sound as a dipole [62]. The cumulative power spectrum of a bubble size distribution is obtained by summing the power spectra of individual bubbles as

$$P(\omega) = \left(\frac{3\gamma p_o}{\rho}\right)^3 \left(\frac{\rho\varepsilon L d}{c}\right)^2 \sum_i \frac{1}{R_i^4} \left\{ \frac{\omega_i^2 \left(\delta - 2kR_i\right)^2 + 4\omega^2}{\left(kR_i\right)^2 \left[\left(\delta\omega_i\right)^2 + 4\left(\omega_i - \omega\right)^2\right]\left[\left(\delta\omega_i\right)^2 + 4\left(\omega_i + \omega\right)^2\right]} \right\} \tag{14}$$

where d is the depth of the hydrophone, and R_i is the distance between the bubble source and the hydrophone. The dipole strength of a bubble is controlled by the product εL, where ε is the fractional amplitude of bubble oscillation ($\varepsilon = da/a$, where a is bubble radius) and L is the displacement in the dipole moment. The dimensionless damping constant $\delta(f) \approx 0.0025 f^{1/3}$ [61] was used in the calculation because it takes into consideration both radiation and thermal damping. The procedure of calculating the sound spectra from bubble size distributions is described in detail in [P VI].

Prior to calculating brackish water spectra, the bubble noise model was used to resolve the bubble size distribution behind a typical spectral slope of 5 to 6 dB/octave, observed in oceanic spectra at frequencies above 1 kHz [35]. Sound spectra were calculated for bubble densities with varying power-law scaling. The synthetic bubble size distributions were proportional to the bubble radius to the power of $-q$, i.e. $n(a) \sim a^{-q}$. A spectral slope of ≈ 5.7 dB/oct (19 dB/dec) was obtained with a bubble density $n(a) \sim a^{-(3/2)}$, see Fig. 7.2. This is a numerical verification of the discovery by Deane

and Stokes [8], where bubbles less than about 1 mm in radius exhibit a bubble density proportional to $a^{-(3/2)}$ as a result of jet and drop impact on the wave face.

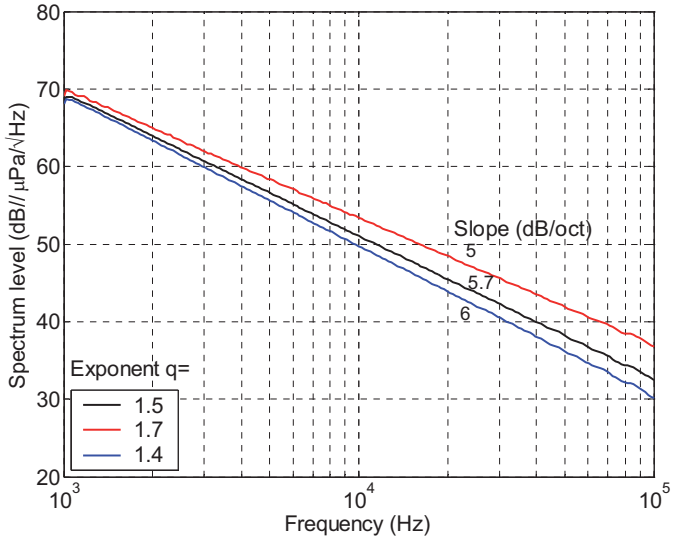

Fig. 7.2: Modeled dependence of sound spectral slope on the slope factor q of the bubble size distribution $n(a) \sim a^{-q}$.

The power-law scaling was varied around -3/2 in order to determine the sensitivity of spectral slope to the slope factor q of the bubble size distribution. The exponent values q= 1.7 and 1.4 in the bubble size distribution correspond to a spectral slope range of 5 to 6 dB/octave, see Fig. 7.2. The levels of the spectra are normalized to intersect at a frequency of 1 kHz, which means that the corresponding bubble size densities are of the same level at larger bubble sizes. The steeper the bubble size distribution (the larger q), the more small bubbles in the distribution, which decreases the spectral slope above 1 kHz.

The measured and modeled spectra for oceanic and brackish water environments are depicted in Fig. 7.3(a). The ocean spectrum corresponds to sea state 6 [2], and the brackish water spectrum is that for 16 m/s, taken from Fig. 5.6. The characteristic dual-slope pattern separates the brackish water spectra from the steadily sloping oceanic spectrum. Relative bubble densities fitted to the spectra are depicted in Fig. 7.3(b). The best fit to the deep-water oceanic spectrum is obtained with $n(a) \sim a^{-(3/2)}$.

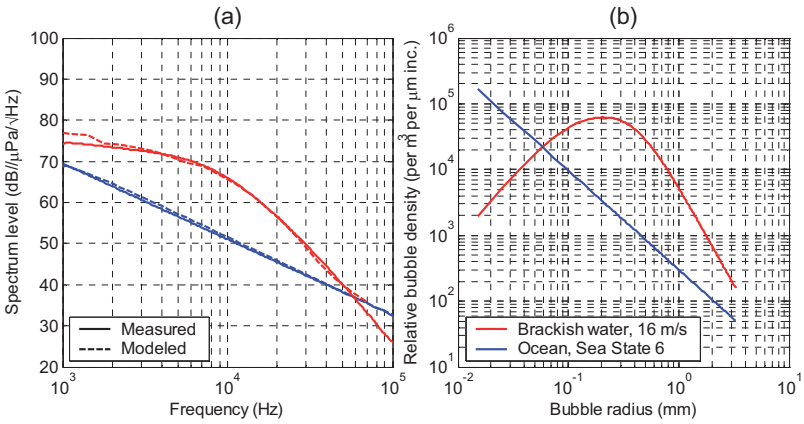

Fig. 7.3: Measured and modelled spectra, and (b) corresponding relative bubble densities. Curve fitting parameters for the brackish water curve at a wind speed of 16 m/s are a_1=0.1 mm, a_2=0.4 mm k_1= 2, and k_2= 3. The ocean spectrum in (a) is for sea state 6 [2].

The bubble size distribution in brackish water develops a distinctive maximum at radii between 0.1 and 0.3 mm, together with a relative drop in bubble density below a radius of 0.1 mm. The pronounced maximum in the brackish water distribution seems to explain the modest spectral slopes at frequencies between 1 - 10 kHz while the steep slopes above 10 kHz are due to the relative scarcity of small bubbles at radii less than 0.1 mm. The complete modeling of brackish water spectra is presented in [P VI].

8 Summary of publications

Publication I

The Finnish Naval Research Institute (FNRI) has conducted hydroacoustic measurements in the Gulf of Finland (GOF) mainly during sea trials of new sonar systems. The physical environment of the Baltic sea area is described: bathymetry, sediment classes, salinity and sea currents are discussed. Most of the measurements were done close to shipping lanes where

the hydroacoustical environment is extremely variable. Long term ambient noise data were collected from fixed bottom mounted hydrophone systems. Ambient noise is presented as a function of wind speed for summer and winter conditions. The results indicate that the ambient noise level with moderate winds is 5 - 10 dB lower in summer than in winter. Averaged seasonal sound speed profiles are also presented for the GOF. Bottom backscattering tests were carried out on two specific sites in the GOF using broadband waveforms. The results show that bottom reverberation falls off slower than predicted by Lambert's law. The hydroacoustic results have been used in optimizing active sonar performance in local environment. According to the sonar equation modelling an optimum sonar should operate at 5 - 10 kHz with the pulse bandwidth of ca 2 kHz and the pulse length between 1 – 2 s.

Publication II

Ambient noise measurements were carried out in very shallow water in the archipelago of The Gulf of Finland during 9 months. The period covered all the seasons excluding the late spring and the early summer, and weather conditions varied from calm sea to near gale winds. A calibrated measurement system with a low-noise preamplifier was designed and optimized for noise measurements. The effect of wind speed on the ambient spectrum is significant at frequencies above 100 Hz and at wind speeds exceeding 2 - 3 m/s. The ambient spectral level around 2 kHz is increased by 11 dB as wind speed is doubled. Any general tendency of the very shallow water levels being higher than those of the deep-water spectra was not found in this study. However, the bandwidths of the measured ambient noise were broader than those of the average deep-water noise. At moderate and high winds the ambient spectra showed the typical deep-water slope of 5 - 6 dB/oct at high frequencies. At frequencies below the maximum level the steep decline of up to 12 dB/oct was discovered. It is well known that the ambient noise spectrum varies significantly from point to point in shallow water environment. This particular site was not corrupted by shipping noise which made it possible to study the wind driven effects on the ambient noise also at lower frequencies. No seasonal effect was observed in the measured spectra.

Publication III

The full-year shallow water ambient noise measurements were carried out in a brackish water environment where the depth of the hydrophone was 15 m. The measurement site was well isolated from traffic noise which made it possible to study wind-generated effects at lower frequencies. Due to the near field conditions the ambient noise levels were not significantly distorted by propagation effects. The ambient noise spectrum levels develop a bubble type bandpass structure above 100 Hz as the wind speed increases. The observed sharp spectral declines below 500 Hz are most likely caused by the resonances of oscillating bubble clouds created by breaking waves. The low frequency range of the declines may be attributed to the larger bubble sizes in fresh and brackish waters.

The ambient noise levels are in fairly good agreement with the average deep water levels for the highest wind speeds but the wind speed dependences differ markedly from each other. In shallow brackish water the wind speed dependence factor at 200 Hz is ~ 2.4 which is significantly higher than the typical factor of ~ 1.5 for the ocean environment. The observed high frequency spectral slope m_1 ~ -5 dB/octave remains fairly constant at all wind speeds but is about 1 dB/octave less than the typical deep water slope of ~ -6 dB/octave. The measurements were carried out in all four seasons of the year but no significant seasonal effects were found in any parameter calculated from the spectra. The preferred explanation for the different spectral characteristics observed in the present data is that the bubble size distribution and sound generating mechanisms in breaking waves differ in the archipelago and ocean environment.

Publication IV

The majority of reported studies on underwater ambient noise is focused on frequencies below 20 kHz. The present ambient noise measurements were carried out in a shallow brackish water environment at the frequency range extending up to 70 kHz. The study is a follow-up to the previous campaign which focused on the low-frequency characteristics of ambient noise. The ambient noise spectra show a distinctive band-limited structure where spectrum levels decline rapidly at both ends of the frequency band, i.e. above 15 to 20 kHz and below 500 Hz. The high-frequency spectral de-

cline above 1 kHz can be divided into two consecutive frequency ranges that have different spectral slopes. The ambient noise spectrum was modeled with a single oscillating bubble model. The transition from a single-slope to a dual-slope pattern is modeled by varying the bubble size distribution, which is known to be different in a saline ocean environment and brackish water. The steeper spectral slope in brackish water above 10 kHz is obtained with the bubble size distribution where bubble densities below a radius of 0.1 mm are markedly lower than those in an ocean environment.

Publication V

The ambient noise measurements were carried out in a shallow brackish water environment over a frequency range extending up to 70 kHz. The measurement site is well isolated against traffic noise and other man-made interferences. The measured ambient noise spectra show a distinctive bandpass structure characteristic of the dipolar source distribution formed by bubbles in breaking waves. The broadband spectra reveal an unexpected feature at frequencies above 10 kHz where the spectral slopes steepen markedly at intermediate and high wind speeds. This is attributed mainly to the threshold wind speed parameter, which increases rapidly at frequencies above 13 kHz. A plausible physical explanation for the observation is that fresh and brackish water are known to contain a lower proportion of small bubbles than salty oceanic water. Bubble sizes required to radiate sound above 10 kHz are less than 0.3 mm in radius. In brackish water it seems that bubbles of this size do not start to develop until the highest wind speeds are attained.

Publication VI

High-frequency ambient noise spectra measured in a shallow brackish water environment exhibits a dual-slope spectral pattern above 1 kHz due to increased attenuation above 10 kHz at intermediate and high wind speeds. The study demonstrates with Commander and Prosperetti's dispersion relation that absorption in brackish and fresh water, unlike in ocean water, tends to decrease above a frequency of 10 kHz due to the low proportion of small bubbles in a bubbly mixture created by breaking waves. The excess high-frequency attenuation in the spectra cannot therefore be directly attributed to the effects of absorption in a bubbly mixture. Measured ambient noise spectra were modeled as a cumulative power spectrum of

individual resonating bubbles distributed in a radius range of 0.01 - 3.3 mm using Loewen and Melville's model for the sound generated by breaking waves. The bubble density of a brackish water spectrum was coupled to that of the average deep-water spectrum, the bubble density of which is well documented in literature. The best fit to the average deep-water spectrum having a spectral slope of 5.7 dB/octave (19 dB/dec) was obtained with a bubble density that is proportional to the bubble radius to the power of -3/2. The dual-slope pattern observed in the brackish water spectra is mostly explained with a bubble size distribution that has a distinctive maximum at radii between 0.1 and 0.3 mm, and a relative drop in bubble density below a radius of 0.1 mm.

9 Conclusions

The shallow water ambient noise measurements were conducted in a brackish water environment where hydrophones were located at depths of 15-20 m. The measurement site was well isolated from traffic noise which made it possible to study wind-generated effects also at lower frequencies. Due to the near-field conditions the ambient noise levels were not significantly distorted by propagation effects. The measured ambient noise spectra show a distinctive bandpass structure characteristic of the dipolar source distribution formed by bubbles in breaking waves. The observed sharp spectral declines below 500 Hz are most likely caused by the resonances of oscillating bubble clouds created by breaking waves. The low frequency range of the declines may be attributed to the larger bubble sizes in fresh and brackish waters compared to saline water.

High-frequency ambient noise spectra exhibit a dual-slope spectral pattern above 1 kHz due to increased attenuation above 10 kHz at intermediate and high wind speeds. The study demonstrates with Commander and Prosperetti's dispersion relation that absorption in brackish and fresh water, unlike in ocean water, tends to decrease above a frequency of 10 kHz due to the low proportion of small bubbles in a bubbly mixture created by breaking waves. The excess high-frequency attenuation in the spectra cannot therefore be directly attributed to the effects of absorption in a bubbly mixture.

Measured ambient noise spectra were modeled as a cumulative power spectrum of individual resonating bubbles distributed in a radius range of

0.01 - 3.3 mm using Loewen and Melville's model for the sound generated by breaking waves. The dual-slope pattern observed in the brackish water spectra is mostly explained with a bubble size distribution that has a distinctive maximum at radii between 0.1 and 0.3 mm, and a relative drop in bubble density below a radius of 0.1 mm. A physical explanation for this is the fact that small bubbles have a tendency to coalesce in fresh and brackish water, while saltwater bubbles repel each other, thus preventing the loss of small bubbles by coalescence.

The best fit to the average deep-water spectrum having a spectral slope of 5.7 dB/octave (19 dB/dec) was obtained with a bubble size distribution that is proportional to the bubble radius to the power of –(3/2). A typical slope range of 5 to 6 dB/octave, reported in literature for oceanic ambient noise spectra, corresponds to the bubble size distribution power factors of -1.7 and -1.4, respectively.

One should, however, be careful not to generalize the present brackish water results too much due to the inherent complexity of a coastal environment. Bubble densities are known to have considerable spatial variability depending on seasonal, biological, and even weather conditions.

References

[1] R.B. Lindsay, *ACOUSTICS: Historical and philosophical development*, Dowden, Hutchinson & Ross, Stroudsburg, PA, 1972.

[2] R.J. Urick, *Principles of underwater sound, 3rd ed.*, Peninsula, Los Altos, CA, 1983.

[3] W.S. Burdic, *Underwater acoustic system analysis, 2nd ed.*, Prentice Hall, Englewood Cliffs, NJ, 1991.

[4] D. Ross, *Mechanics of underwater noise*, Prentice Hall, Peninsula, Los Altos, CA, 1987.

[5] W.J. Richardson, C.R Greene Jr., C.I. Malme, and D.H. Thomson, *Marine mammals and noise*, Academic Press, San Diego, CA, 1995.

[6] E. McCarthy, *International regulation of underwater sound: Establishing rules and standards to address ocean noise pollution*, Kluwer, Boston, MA, 2010.

[7] E. Traer, P. Gerstoft, and W.S. Hodgkiss, “Ocean bottom profiling with ambient noise: A model for the passive fathometer,” *J. Acoust. Soc. Am.*, vol. 129, no. 4, pp. 1825-1836, 2011.

[8] G.B. Deane, and M.D. Stokes, ”Scale dependence of bubble creation mechanisms in breaking waves,” *Nature*, vol. 418, pp. 839-844, 2002.

[9] M. Lasky, “Review of undersea acoustics to 1950,” *J. Acoust. Soc. Am.*, vol. 61, no. 2, pp. 283-297, 1977.

[10] M. Klein, “Underwater sound and naval acoustical research before 1939,” *J. Acoust. Soc. Am.*, vol. 43, no. 5, pp. 931-947, 1968.

[11] Sonar: http://en.wikipedia.org/wiki/Sonar

[12] L.E. Holt, “German use of sonic listening,” *J. Acoust. Soc. Am.*, vol. 19, no. 4, pp. 678-681, 1947.

[13] M. Minnaert, “On musical air bubbles and the sound of running water,” Philos. Mag., vol. 16, pp. 235-248,1933.

[14] O. Knaapi, “Vesikuuntelulaitteet, teknilliset ominaisuudet ja taktillinen käyttö,” *Sotakorkeakoulu VO1 (National Defence University)*, unpublished diploma thesis, 1948, (In Finnish).

[15] V.O. Knudsen, R.S., Alford, and J.W. Emling, “Underwater ambient noise, ” *J. Mar. Res.*, vol. 7, pp. 410-429, 1948.

[16] X. Lurton, *An introduction to underwater acoustics*, Springer/Praxis, Chichester, UK, 2002.

[17] Marine mammals and Sonar: http://en.wikipedia.org/wiki/Marine_mammals_and_sonar

[18] W.W.L. Au, and M.C. Hastings, *Principles of marine bioacoustics*, Springer, New York, 2010.

[19] P.O. Ekman, *Sukellusvenesotaa Itämerellä*, Merikustannus Oy, Helsinki, 1983, (In Finnish).

[20] O. Enqvist, *Mäkiluoto*, Suomenlinnan rannikkotykistökilta r.y./FORTECA, Przasnysz, Poland, 2007, (In Finnish).

[21] A.O. Bauer, “Some hardly known aspects of the GHG, the U-boat’s group listening apparatus,” 1996, available at: http://www.xs4all.nl/~aobauer/sonar-ghg.htm .

[22] L.E. Kinsler, A.B. Coppens, A.R. Frey, and J.V. Sanders, *Fundamentals of acoustics, 3rd ed.*, Wiley, NJ, 1982.

[23] P.C. Etter, *Underwater acoustic modeling: Principles, techniques and applications, 2nd ed.* , E & FN SPON (Chapman & Hall), London, 1991.

[24] H. Hollien and J.F. Brandt, "Effect of air bubbles in the external auditory meatus on underwater hearing thresholds," *J. Acoust. Soc. Am.*, vol. 46, no. 2, pp. 384-387, 1969.

[25] D.A. Norman, R. Phelps, and F. Wightman, "Some observations on underwater hearing," *J. Acoust. Soc. Am.*, vol. 50, no. 2, pp. 544-548, 1971.

[26] H. Hollien, and S. Feinstein, "Contribution of the external auditory meatus to auditory sensitivity underwater," *J. Acoust. Soc. Am.*, vol. 57, no. 6, pp. 1488-1492, 1975.

[27] J. Zwislocki, "In search of the bone-conduction threshold in a free sound field," *J. Acoust. Soc. Am.*, vol. 29, no. 7, pp. 795-804, 1957.

[28] S. Savel, C. Drake, and G. Rabau, "Human auditory localization in a distorted environment: Water," *Acta Acustica united with Acustica*, vol. 95, no. 1, pp. 128-141, 2009.

[29] S.J. Parvin, "The effect of low frequency underwater sound on divers," In *Proc. Undersea Defence Technology (UDT)*, Wembley, UK, 1998, pp. 227-232.

[30] J.R. Nedwell, B. Edwards, and A.W.H. Turnpenny, and J. Gordon, "Fish and marine mammal audiograms: A summary of available information," Subacoustech report ref# 534R0214, 2004, available also at http://www.subacoustech.com/information/publications.shtml .

[31] P.H. Dahl, J.H. Miller, D.H. Cato, and R.K. Andrew, "Underwater ambient noise," *Acoustics Today*, vol. 3, no. 1, pp. 23-33, 2007.

[32] R.H. Stewart, *Introduction to physical oceanography*, Texas A&M University, 2008. Open source textbook available at http://oceanworld.tamu.edu/resources/ocng_textbook/contents.html .

[33] J. Wu, "Wind-Stress coefficients over sea surface near neutral conditions – A revisit," *," J. Phys. Oceanogr.*, vol. 10, pp. 727-740, 1980.

[34] W.M. Carey, and R.B. Evans, *Ocean ambient noise*, Springer, New York, 2011.

[35] G.M. Wenz, “Acoustic ambient noise in the ocean: Spectra and sources,” *J. Acoust. Soc. Am.*, vol. 34, no. 12, pp. 1936-1956, 1962.

[36] R.J. Urick, *Ambient noise in the sea*, Peninsula, Los Altos, CA, 1984.

[37] G.J. Franz, “Splashes as sources of sound in liquids ,” *J. Acoust. Soc. Am.*. vol. 31, no. 8, pp. 1080-1096, 1959.

[38] R.H. Mellen, “The thermal-noise limit in the detection of underwater acoustic signals,” *J. Acoust. Soc. Am.*, vol. 24, no. 5, pp. 478-480, 1952.

[39] Ocean Studies Board (OSB)/National Research Council (NRC), *Ocean noise and marine mammals*, The National Academic Press, 2003. Available at http://www.nap.edu/catalog.php?record_id=10564.

[40] B.R. Kerman, “Underwater sound generation by breaking wind waves,” *J. Acoust. Soc. Am.*, vol. 75, no. 1, pp. 149-165, 1984.

[41] W.M. Carey, and D. Browning, “Low frequency ocean ambient noise: measurements and theory,” in *Natural mechanisms of surface generated noise in the ocean*, ed. B. R. Kerman, Kluwer, Dordrecht, The Netherlands, 1988, pp. 361-376.

[42] W.M. Carey, and J.W. Fitzgerald, “Low frequency noise from breaking waves,” in *Sea Surface Sound (2): Natural Physical Sources of Underwater Sound*, ed. B. R. Kerman , Kluwer, Dordrecht, The Netherlands, 1993, pp. 277-304.

[43] A. Prosperetti, “Bubble-related ambient noise in the ocean,” *J. Acoust. Soc. Am.*, vol. 84, no. 3, pp. 1042-1054, 1988.

[44] S.W. Yoon, L.A. Crum, A. Prosperetti, and Q. Lu, “An investigation of the collective oscillations of a bubble cloud,” *J. Acoust. Soc. Am.*, vol. 89, no. 2, pp. 700-706, 1991.

[45] W.M. Carey, J.W. Fitzgerald, E.C. Monahan, and Q. Wang, “Measurement of the sound produced by a tipping trough with fresh and salt water,” *J. Acoust. Soc. Am.*, vol. 93, no. 6, pp. 3178-3192, 1993.

[46] M.Y. Su, and J. Cartmill, “Effects of salinity on breaking wave generated void fraction and bubble size spectra,” in *Proceedings of Air-Water Gas Transfer*, eds. B. Jähne and E. Mohanan (AEON Verlag), pp. 305-311, 1995.

[47] E.S. Winkel, S.L. Ceccio, D.R. Dowling, and M. Perlin, “Bubble-size distributions produced by wall injection of air into flowing freshwater,

saltwater and surfactant solutions," *Experiments in Fluids*, vol. 37, pp. 802-810, 2004.

[48] A.R. Kolaini, "Sound radiation by various types of laboratory breaking waves in fresh and salt water," *J. Acoust. Soc. Am.*, vol. 103 ,no. 1, pp. 300-308, 1998.

[49] G.J. Orris, and M. Nicholas, "Collective oscillations of fresh and salt water bubble plumes," *J. Acoust. Soc. Am.*, vol. 107, no. 2, pp. 771-787, 2000.

[50] Thorpe, and Stubbs, "Bubbles in a freshwater lake," *Nature*, vol. 279, pp. 403-405, 1979.

[51] G. Kullenberg, "Physical oceanography," in *The Baltic Sea,* ed. A. Voipio, Elsevier Oceanography Series, 30, Elsevier, Amsterdam, The Netherlands, pp. 135-181, 1981.

[52] P.C. Wille, and D. Geyer, "Measurements on the origin of the wind-dependent ambient noise variability in shallow water," *J. Acoust. Soc. Am.,* vol. 75, no. 1, pp. 173-185, 1984.

[53] R. Wagstaff, and J. Newcombe, "Omnidirectional ambient noise in the Southern Baltic Sea" in *Progress in underwater acoustics*, ed. H. Merklinger, Plenum Press, New York, London, 1987.

[54] Z. Klusek, and A. Lisimenka, "Ambient sea noise in the Baltic Sea," In *Proceedings of the 2nd International Conference on Underwater Acoustic Measurement: Technologies and Results (UAM 2007)*, Heraklion, Greece, June 25-29, 2007.

[55] J. Pihl, J-O. Hegethorn, S. Ivansson, P. Moren, E. Norrbrand, B. Nilsson, G. Sundin, A. Wester, and V. Westerlin, "Underwater acoustics in the Baltic", *Swedish Defense Research Agency (FOI)*, report FOA-R—98-00727-409—SE, 1998.

[56] E. Dahlberg, R. Lennartsson, M. Levonen, L. Persson, "Properties of acoustic ambient noise in the Baltic Sea," In *Proceedings of the 1st International Conference on Underwater Acoustic Measurement: Technologies and Results (UAM 2005)*, Heraklion, Greece, June 28-July 1, 2005.

[57] A.V. Oppenheim, R.W. Schafer, *Digital signal processing*, Prentice-Hall, New Jersey, U.S.A., 1975.

[58] C. L. Piggott, “Ambient sea noise at low frequencies in shallow water of the Scotian Shelf,” *J. Acoust. Soc. Am.*, vol. 36, no. 11, pp. 2152-2163, 1964.

[59] G.B. Deane, ”Sound generation and air entrainment by breaking waves in the surf zone,” *J. Acoust. Soc. Am.,* vol. 102, no. 5, pp. 2671-2689, 1997.

[60] K.W. Commander, and A. Prosperetti, ”Linear pressure waves in bubbly liquids: Comparison between theory and experiments,” *J. Acoust. Soc. Am.*, vol. 85, no. 2, pp. 732-746, 1989.

[61] H. Medwin, and C.S. Clay, *Fundamentals of acoustical oceanography*, Academic Press, San Diego, CA, 1998.

[62] M.R. Loewen, and W.K. Melville, ”A model of the sound generated by breaking waves,” *J. Acoust. Soc. Am.*, vol. 90, no. 4, pp. 2075-2080, 1991.

Figure on the front cover is the spectrogram of a sound signal measured on the bottom of the sea while a broadband underwater sound source passes the hydrophone. The interference pattern in the figure is the Lloyd's mirror effect, which arises from constructive and destructive interference between direct and surface-reflected sound waves.

Aalto-DD 18/2012

ISBN 978-952-60-4513-9
ISBN 978-952-60-4514-6 (pdf)
ISSN-L 1799-4934
ISSN 1799-4934
ISSN 1799-4942 (pdf)

Aalto University
School of Electrical Engineering
Department of Signal Processing and Acoustics
www.aalto.fi

BUSINESS + ECONOMY

ART + DESIGN + ARCHITECTURE

SCIENCE + TECHNOLOGY

CROSSOVER

DOCTORAL DISSERTATIONS